Sapkota, K., Irvine, M. W., Fang, G., Burnell, E. S., Bannister, N., Volianskis, A., ... Monaghan, D. T. (2017). Mechanism and properties of positive allosteric modulation of N-methyl-d-aspartate receptors by 6-alkyl 2-naphthoic acid derivatives. *Neuropharmacology*, *125*, 64-79. https://doi.org/10.1016/j.neuropharm.2017.07.007

Keywords

L-glutamate

N-methyl-D-aspartate

Potentiator

Positive allosteric modulator

Deactivation

Ligand-binding domain

I. Introduction

The primary excitatory neurotransmitter in the vertebrate CNS, L-glutamate, activates three distinct families of ligand-gated ion channel receptors that are named for agonists by which they are selectively activated, *N*-methyl-D-aspartate (NMDA), (*S*)-2-amino-3-hydroxy-5-methyl-4-isoxazole propionic acid (AMPA) and kainate (Monaghan et al., 1989; Watkins and Evans, 1981; Watkins et al., 1990). While AMPA and kainate receptors underlie fast excitatory synaptic transmission in the CNS, NMDA receptors (NMDARs) activate relatively slow currents that trigger multiple calcium-dependent intracellular responses that play key roles in learning, memory, and cognition. Excessive NMDAR activation contributes to neuronal cell death in stroke, traumatic brain injury and various neurodegenerative diseases (Kamat et al., 2016; Koutsilieri and Riederer, 2007; Pivovarova and Andrews, 2010), whereas too little NMDAR activity impairs CNS function and, in particular, may cause symptoms seen in schizophrenia and autism (Coyle, 2006; Kantrowitz and Javitt, 2010; Lisman et al., 2008). Thus, the recent development of agents that augment NMDAR activity (positive allosteric modulators, or PAMs) offers an alternative approach for treating neuropsychiatric disorders such as schizophrenia that are not fully managed by currently available therapies. Of the genetic defects associated with schizophrenia, some would be expected to cause global NMDAR hypofunction – for example a defect in D-serine racemase (Luykx et al., 2015; Schizophrenia Working Group of the Psychiatric Genomics, 2014), whereas other defects would be expected to affect subpopulations of NMDARs such as defects in genes which code for individual NMDAR subunits (Greenwood et al., 2012; Sun et al., 2010). Thus, global and subtype-specific NMDAR PAMs may each have patient-specific indications.

NMDAR complexes are composed of subunits from seven genes - GluN1, GluN2A-GluN2D, and GluN3A-GluN3B (Ishii et al., 1993; Mishina et al., 1993; Monyer et al., 1994). These subunits assemble into hetero-tetrameric complexes in various combinations resulting in functionally-distinct NMDARs. Many NMDARs are thought to be composed of two GluN1 subunits and two GluN2 subunits. The different alternatively spliced GluN1 isoforms have largely similar pharmacological and physiological properties whereas the GluN2 subunits confer distinct physiological, biochemical, and pharmacological properties to the NMDAR complex (Buller et al., 1994; Hollmann et al., 1993; Ikeda et al., 1992; Monyer et al., 1994; Sugihara et al., 1992; Vicini et al., 1998). These properties, combined with their varied developmental profiles and anatomical distributions (Watanabe et al., 1992, 1993), imply that GluN2 subtype-selective agents would have distinct physiological and therapeutic properties.

Previously we have reported multiple aromatic ring structures substituted with a carboxylic acid group that display NMDAR PAM and/or NAM activity with varied patterns of subunit selectivity (Costa et al., 2012; Costa et al., 2010; Irvine et al., 2012; Irvine et al., 2015). These agents are allosteric modulators interacting at the ligand binding domain (LBD) but they do not compete with either glutamate or glycine binding, nor do they bind at the *N*-terminal regulatory domain or within the ion channel (Costa et al., 2010). In contrast to agents that potentiate NMDARs containing specific GluN2 subunits, e.g. pregnenalone sulphate (PS) (Horak et al., 2006), UBP710 - GluN2A/GluN2B; UBP512 - GluN2A (Costa et al., 2010); GNE-8324 - GluN2A (Hackos et al., 2016); CIQ – GluN2C/GluN2D (Mullasseril et al., 2010); PYD-106 – GluN2C (Khatri et al., 2014), the phenanthroic acid derivative UBP646 (Costa et al.,

2010) and the cholesterol derivative SGE-201 (Paul et al., 2013) potentiate all four GluN1/GluN2 subtypes. Thus, in cases where it would be useful to augment global NMDAR function, agents with these properties may be beneficial.

In this study, we characterize the functional properties of two naphthoic acid derivatives related to UBP646 which robustly enhance currents at each of the four GluN1/GluN2 NMDARs, UBP684 (6-(4-methylpent-1-yl)-2-naphthoic acid) and UBP753 ((*RS*)-6-(5-methylhexan-2-yl)-2-naphthoic acid). We also identify mechanisms by which these agents can enhance NMDAR currents.

2. Methods

2.1 Compounds

UBP684, UBP753 and UBP792 ((*E*)-3-hydroxy-7-(2-nitrostyryl)-2-naphthoic acid) were synthesized and their structures were confirmed by ^{1}H- and ^{13}C-nuclear magnetic resonance (NMR) as well as mass spectroscopy. All compounds had elemental analyses where the determined percentage of C, H and N were less than 0.4 % different from theoretical values. Details of synthesis and purification will be reported elsewhere. Stock solutions were prepared in dimethyl sulfoxide at a concentration of 50 mM. The working solution was prepared in recording buffer just before the experiment. Other chemicals were obtained from Sigma unless stated otherwise.

2.2 GluN1 Subunit Expression in Xenopus oocytes

cDNA encoding the NMDAR GluN1-1a subunit was a generous gift of Dr. Shigetada Nakanishi (Kyoto, Japan). cDNA encoding the GluNA, GluN2C and GluN2D subunits were kindly provided by Dr. Peter Seeburg (Heidelburg, Germany) and the

GluN2B [5' UTR] cDNA was the generous gift of Drs. Dolan Pritchett and David Lynch (Philadelphia, USA). GluN1 and GluN2A constructs with cysteine substitution at N499C and Q686C in GluN1 (hereafter GluN1^{C}) and at K487C and N687C in GluN2A (hereafter GluN2A^{C}) were kindly provided by Dr. Gabriela Popescu (University of Buffalo, USA). Plasmids were linearized with Not I (GluN1a, GluN1^{C}, GluN2A^{C}), EcoR I (GluN2A, GluN2C and GluN2D) or Sal I (GluN2B) and transcribed in vitro with T3 (GluN2A, GluN2C), SP6 (GluN2B) or T7 (GluN1a, GluN2D) RNA polymerase using mMessage mMachine transcription kits (Ambion, Austin, TX, USA).

Oocytes were removed and isolated from mature female *Xenopus laevis* (Xenopus One, Ann Arbor, MI, USA) as previously described (Buller *et al*., 1994). Procedures for animal handling were approved by the University of Nebraska Medical Center's Animal Care and Use Committee in compliance with the National Institutes of Health guidelines. NMDAR subunit RNAs were dissolved in sterile distilled H_2O. GluN1a and GluN2 RNAs were mixed in a molar ratio of 1:3. 50 nl of the final RNA mixture was microinjected (15-30 ng total) into the cytoplasm of oocyte. Oocytes were incubated in ND-96 solution at 17°C prior to electrophysiological assay (1-5 days).

2.3 Two electrode voltage clamp electrophysiology

Electrophysiological responses were measured using a standard two-microelectrode voltage clamp (Warner Instruments, Hamden, Connecticut, model OC-725B) designed to provide fast clamp of large cells. The recording buffer contained (mM) 116 NaCl, 2 KCl, 0.3 $BaCl_2$, 5 mM 4-(2-hydroxyethyl)-1-piperazineethanesulfonic acid (HEPES), 0.005 EGTA (or 0.01 diethylenetriaminepentaacetic acid, DTPA), and pH was adjusted to 7.4. Response magnitude was determined by the steady-state plateau response elicited by bath

application of 10 μM L-glutamate plus 10 μM glycine at a holding potential of –60 mV unless stated otherwise. Response amplitudes for the four heteromeric complexes were generally between 0.2 to 1.5 μA. Compounds were bath applied in recording buffer (Automate Scientific 8- or 16-channel perfusion system) and the responses were digitized for quantification (Digidata 1440A and pClamp-10, Molecular Devices). Dose-response relationships were fit to a single-site (GraphPad Prism, ISI Software, San Diego, CA, USA), using a nonlinear regression to calculate IC_{50} or EC_{50} and % maximal response.

2.4 Hippocampal neuron whole-cell patch clamp recordings.

Whole-cell electrophysiology was conducted as previously described (Chopra et al., 2015). Briefly, mice (~30-35 day old) were anesthetized by isoflurane and decapitated in accordance with the approved protocols of Creighton University IACUC. The brain was rapidly removed and placed in ice-cold artificial cerebrospinal fluid (ACSF) of the following composition (in mM): 130 NaCl, 24 $NaHCO_3$, 3.5 KCl, 1.25 NaH_2PO_4, 0.5 $CaCl_2$, 3 $MgCl_2$ and 10 glucose saturated with 95% O_2/5% CO_2. 300 μm thick sagittal sections were prepared using vibrating microtome (Leica VT1200, Buffalo Grove, IL, USA). Whole-cell patch recordings were obtained from CA1 pyramidal neurons in voltage-clamp configuration at +40 mV with an Axopatch 200B (Molecular Devices, Sunnyvale, CA, USA). Glass pipette with a resistance of 5–8 mOhm were filled with an internal solution consisting of (in mM) 110 cesium gluconate, 30 CsCl, 5 HEPES, 4 NaCl, 0.5 $CaCl_2$, 2 $MgCl_2$, 5 BAPTA,2 Na_2ATP, and 0.3 Na_2GTP (pH 7.35). Slices in the recording chamber were initially maintained in artificial cerebrospinal fluid (ACSF) containing 1.5 mM $CaCl_2$ and 1.5 mM $MgCl_2$. NMDAR responses were then recorded in ACSF in the presence of 0.5 μM tetrodotoxin, 100 μM picrotoxin and 10 μM NBQX with

and without UBP684 in calcium-free recording buffer to improve compound solubility. Signal was filtered at 2 kHz and digitized at 5 kHz using an Axon Digidata 1440A analog-to-digital board (Molecular Devices, CA). NMDAR responses were obtained by briefly applying agonists (100 μM NMDA + 100 μM glycine) dissolved in the extracellular buffer using a Picospritzer II. The application duration ranged from 30-50 ms. UBP684 (60 μM) was applied to the bath solution and changes in agonist responses were noted.

2.5 HEK cell patch-clamp recordings

Cell transfection and electrophysiology were performed as described previously (Bresink et al., 1996). Briefly, HEK 293 cells were transfected with GluN1a and GluN2A in the presence of 5 μg of eGFP (enhanced Green Fluorescent Protein) DNA in order to aid visualization of the transfected cells. Electrophysiological experiments were performed at room temperature. External bath solution contained (in mM): 145 NaCl, 2 KCl, 10 HEPES, 10 Glucose, 0.5 $CaCl_2$, 0.01 EDTA, 0.05 Glycine. Internal pipette solution contained (in mM): 110 Cs Gluconate, 5 HEPES, 0.5 $CaCl_2$, 2 Mg ATP, 0.3 mM Na GTP, 30 $CsCl_2$, 8 NaCl, 5 BAPTA; pH 7.35. Cells were visualized using a 20 x objective and phase contrast optics on an inverted microscope (Nikon, Japan). Epifluorescence of the cells expressing eGFP was excited using standard fluorescein filters and most of the cells expressing eGFP gave strong glutamate-mediated responses. Rapid application of glutamate and glycine was achieved using a 2-barreled theta glass pipette driven by a piezoelectric translator (Burleigh). NMDAR-mediated currents were recorded in either whole-cell or outside-out patch-clamp mode (Multiclamp 700A, Axon), digitized and

stored on a PC for off-line analysis (Signal software, Cambridge Electronic Design Limited).

2.6 Data analysis

The association time constant (K_{ON}) of UBP753, was calculated by determining the association time (τ_{ONSET}) of L-glutamate/glycine-evoked current responses at different concentrations of UBP753 that were fit with a single exponential. Linear regression analysis of a plot of $1/\ \tau_{ONSET}$ versus UBP753 concentration gave the K_{ON} (slope) and K_{OFF} (y-intercept) values which were used to calculate the K_D ($K_D=K_{OFF}/K_{ON}$).

2.7 Statistical analyses

All values are expressed as mean ± SEM. Paired and unpaired t-test was used for comparing two numbers and comparisons with more than 2 groups were evaluated by one-way *ANOVA* followed by a Tukey's or Bonferroni's multiple comparison test. Comparisons were considered as statistically significant if $p < 0.05$.

3. Results

3.1 The effects of agonists on PAM activity and of PAMs on agonist activity

The ability of a PAM to potentiate NMDARs can depend upon the effect of agonist concentrations on PAM activity. And in a reciprocal manner, PAM binding can alter agonist activity. Thus, we determined the effect of different agonist concentrations on PAM activity. UBP684 dose-response relationships were determined for the potentiation of GluN2A-D NMDAR responses evoked by 10 μM L-glutamate /10 μM glycine or by 300 μM L-glutamate / 300 μM glycine (Fig. 1, Table 1). UBP684 potentiated responses to low agonist concentrations at each of the NMDAR types with similar EC_{50}s of approximately 30 μM and a maximal potentiation of 69 to 117 % (Table 1). In the presence of high agonist concentrations (Fig. 1C), UBP684 retained its ability to potentiate NMDAR responses. The degree of maximal potentiation was not significantly changed at GluN1a/GluN2A, GluN1a/GluN2C, and GluN1a/GluN2D receptor subtypes and was decreased by 40% at GluN1a/GluN2B receptors. High agonist concentrations enhanced UBP684 potency at receptors containing GluN2A and GluN2B subunits as reflected by a 63% and 28% reduction in EC_{50}, respectively (Table 1), while UBP684 potency at the GluN2D subtype was lowered (93% increase in the EC_{50}).

To determine if UBP684 has PAM activity at native NMDARs, we briefly applied 100 μM NMDA plus 100 μM glycine to CA1 pyramidal cells in hippocampal slices from 1 month-old mice. We found that bath application of UBP684 significantly increased the amplitude of agonist-induced currents (99.0 ± 34.7 % potentiation, $p = 0.046$, t-test) relative to the initial agonist response (Figure 1D). The potentiation was fully reversible with no detectible potentiation after UBP684 washout (-3.6 ± 8.3 % potentiation. The potentiated response was significantly different from the washout condition ($p = 0.021$).

To further define the effect of the PAMs on agonist responses, we determined the effect of 50 μM UBP684 on the dose-response relationship for L-glutamate and for glycine (Fig. 2, Table 2). Depending upon the subunits studied, PAM activity was associated with small shifts in agonist potencies as well as an increase in the maximal response to both agonists. UBP684 increased L-glutamate potency (32% reduction in L-glutamate EC_{50}), but not glycine potency at GluN2A-containing receptors. In contrast, at GluN2B-containing receptors, UBP684 increased glycine potency (30% reduction in glycine EC_{50}), but not L-glutamate potency (Fig. 2 and Table 2). Since UBP684 increases glycine potency, then it is expected that UBP684 would increase GluN1/GluN2B responses more at low glycine concentrations than at high glycine concentrations. This is consistent with the partial reduction we observed in the maximum potentiation of GluN1a/GluN2B responses by UBP684 when high agonist concentrations were used (Table 1). In contrast, at GluN2C- and GluN2D-containing receptors, UBP684 reduced L-glutamate potency (58% and 59% increase in EC_{50}, respectively) and did not significantly change glycine potency (Table 2). Overall, and consistent with the low / high agonist concentration experiments, UBP684 increases the maximal effect of both agonists at all NMDARs at saturating agonist concentrations and additionally has minor, subtype-specific effects on agonist potencies.

UBP753 has an apparent potency that is similar to that of UBP684 and effectively potentiates all four GluN1/GluN2 receptors (Table 1; Fig. 3). However, the limited solubility of UBP753 at concentrations above 100 μM made it difficult to establish saturating conditions to accurately define the EC_{50}. To independently estimate potency, UBP753 on-rate and off-rates were determined at different concentrations (Fig. 3B). The

resulting rate constants indicated a Kd of 73 μM for UBP753 that was 2-fold higher than the EC_{50} for UBP753 estimated by concentration-response analysis. Of relevance to other experiments described below (section 3.2), the slow, dose-dependent on-rates, and dose-independent off-rates for UBP753 indicate that UBP753 binding/unbinding is significantly slower than the solution turnover time.

The ability of UBP684 to reduce L-glutamate potency at GluN1/GluN2D was unexpected for a PAM, although consistent with the greater PAM activity seen with high agonist concentrations (Table 1). Thus, we also evaluated UBP753, for its effect on agonist activity at GluN1a/GluN2D receptors. Like UBP684, UBP753 decreased L-glutamate potency (Fig. 3, Table 2) and had no effect on glycine potency. UBP753 increased both the maximal glycine response and the maximal L-glutamate response.

3.2 PAM potentiation is not use-dependent

The ability of a PAM to potentiate NMDAR responses can also be a function of receptor state. For example, neurosteroids preferrentially bind to the agonist-unbound, inactive receptor state rather than to the active receptor state resulting in "disuse-dependent" PAM activity (Horak et al., 2004). To determine if the PAMs can bind to the inactive receptor state as well as the active state, we evaluated PAM potentiation using different drug-application paradigms (Horak et al., 2004). When UBP753 or UBP684 was applied prior to agonist application, the subsequent GluN1/GluN2B NMDAR agonist response was immediately and fully potentiated (Fig. 4A). This was seen when either applying the PAM alone followed by agonist alone (sequential application), or by pre-applying the PAM followed by PAM co-application with agonist (pre & coapplication). The on-rate of PAM potentiation when it was applied after attaining a steady-state

agonist response (cotemporaneous application) was significantly slower than the agonist alone on-rate. Thus, if agonist binding was required for the PAM to access its binding site, then the onset rate of the agonist response in the pre-coapplication condition should be significantly slower than the agonist alone onset rate – which it was not. Likewise, agonist activation was rapid in the sequential application condition and the magnitude of initial potentiation was not decreased compared to the cotemporaneous application. Co-application of agonist and PAM without prior PAM exposure gave an intermediate initial rate of activation consistent with a rapid agonist action combined with a slower PAM binding and potentiation (Fig. 4A, B). These results suggest that UBP753 and UBP684 can bind to the agonist-unbound state of the NMDAR in addition to the agonist-bound, active state. Unlike the neurosteroid PS (Horak et al., 2004), the degree of potentiation was similar for the different drug application paradigms (Fig. 4C).

3.3 pH Dependence of PAM activity

We determined the effect of pH on PAM activity for two reasons. One is that under pathological conditions such as hypoxia and schizophrenia, the extracellular pH in the brain can change (Chesler and Kaila, 1992; Halim et al., 2008; Siesjo, 1985) which in turn can change the effect of NMDAR modulators (Kostakis et al., 2011; Mott et al., 1998). Secondly, as exemplified by the potentiating actions of spermine on NMDARs (Traynelis et al., 1995), reversing proton inhibition is a potential mechanism of action for an NMDAR PAM. As shown in Fig. 5B, UBP684 was an effective PAM at each of the NMDARs at pH 7.4, but was inhibitory at pH 8.4, with very weak inhibitory effects at receptors containing GluN2A and progressively greater inhibition at NMDARs with GluN2B, GluN2C, and GluN2D subunits. For comparison, we evaluated UBP753 at

GluN1a/GluN2C (Fig. 5C) and found that, like UBP684, UBP753 inhibited NMDAR responses at pH 8.4 and potentiated responses at pH 7.4. Further decreasing the pH to 6.4 resulting in yet greater potentiation.

Given the unexpected inhibitory activity we observed for UBP684 and UBP753 at alkaline pH, we compared this activity to other, structurally-distinct PAMs (Fig. 5D-F). The neurosteroid PS potentiated GluN1a/GluN2A and GluN1a/GluN2B receptor responses at pH 7.4, but this activity was significantly reduced (~50%) at pH 8.4. Similarly, the potentiating effect of CIQ, a GluN1/GluN2C/D PAM, was also significantly reduced at pH 8.4. Thus, unlike UBP684/753, neither PS nor CIQ displayed NAM activity at pH 8.4. The GluN2A-selective PAM GNE-8324, on the other hand, was like UBP684/753 and did display inhibitory activity at pH 8.4 (Fig. 5F).

We next determined if the compounds are affecting the sensitivity of NMDARs to UBP in a manner similar to that seen for spermine potentiation of NMDARs which can be described as a decrease in proton inhibition (or relief of proton block) (Traynelis et al., 1995). Thus, spermine is an effective GluN1a/GluN2B potentiator at acidic pHs (where high proton concentrations inhibit NMDAR function), but at alkaline pH spermine is a weak potentiator. Consequently, spermine potentiation corresponds to a reduction in the ability of protons to inhibit GluN1a/GluN2B receptor responses and thus increases the proton IC_{50}. Thus, we wanted to determine the effect of UBP684 (50 μM) on proton inhibition of GluN1a/GluN2B receptor responses and to compare this to GluN1/GluN2D responses which behaved differently in Fig. 5B. At both receptor types, there was a reduction in the inhibitory potency of protons in the presence of the PAM (Fig. 6). Consistent with Fig. 5B, at pH 8.4, UBP684 not only had a reduced potentiation but

caused inhibition in the receptor response at GluN2D-containing receptors (~50% inhibition) (Fig. 6B). And this inhibition was greater than at receptors containing GluN2B subunits (~25% inhibition). Interestingly, in the pH range 7.0-7.4, UBP684 potentiated GluN1a/GluN2D NMDAR responses well above those seen for the alkaline pH control-response where there is little proton inhibition. Without UBP684, increasing proton concentration from pH 7.4 to 7.0 inhibits the NMDAR response, whereas in the presence of UBP684, increasing proton concentration increased the response. This proton-dependent potentiation in the presence of UBP684 was not seen for GluN1a/GluN2B receptors, which only displayed a reduction in the proton sensitivity (a right-shift in the proton inhibition curve, Fig. 6A). Thus, UBP684 appears to reduce proton inhibition at both GluN2B and GluN2D-containing receptors, but at GluN2D-containing receptors UBP684 has an additional proton-dependent potentiation.

Since UBP684 potentiation is sensitive to pH, we evaluated the effect on PAM activity of the 21 amino acid insert in the GluN1 N-terminal domain that is coded for by exon 5. This insert reduces spermine potentiation by possibly interacting with the N-terminal proton sensor (Traynelis et al., 1995). The presence of this insert also reduces PYD-106 potentiation of GluN1/GluN2C receptors (Khatri et al., 2014) while enhancing PS potentiation of GluN1/GluN2A receptor responses and enhancing PS inhibition of GluN1/GluN2D receptors (Kostakis et al., 2011). To evaluate the effect of the N-terminal insert on both the PAM and NAM activities of UBP684, we evaluated the effect of UBP684 on responses at GluN1a/GluN2D (- exon 5) and GluN1b/GluN2D (+ exon 5) receptors at pH 7.4 and 8.4. At pH 7.4, UBP684 PAM activity was unchanged by the N-terminal insert (Fig. 6C). At pH 8.4, UBP684 NAM potency was weakly increased (from

IC_{50} ~30 μM to ~20 μM) by inclusion of exon 5 (Fig. 6D). Thus, unlike spermine, PS, and PYD-106, the N-terminal insert did not affect UBP684's PAM activity, but it did enhance NAM potency as seen with PS.

3.4 The effect of redox state and membrane potential on PAM activity

In addition to pH, redox potential also modulates NMDAR function. Reduction of cysteine residues by the addition of dithiothreitol (DTT) potentiates NMDAR responses (Kohr et al., 1994; Sullivan et al., 1994). Thus, it is possible that UBP684/753 cause a similar conformational change without needing to change the oxidation state of the receptor or that these two sites interact. We compared the PAM potentiating activity before and after treatment of GluN2D-containing NMDARs with 3 mM DTT for 3 min followed by a one-minute wash. As reported by others, DTT exposure caused a 70.7 ± 9.8 % (n = 9) increase in L-glutamate/glycine-evoked GluN1/GluN2D responses. For both UBP684 and UBP753, the magnitude of potentiation were unaffected by prior exposure to DTT (Fig. 7). Similar results were also found for GluN1/GluN2A receptors (data not shown). Consequently, the potentiation by UBP684/UBP753 appears to be independent of the cysteine reduction potentiation mechanism. The PAM activity of UBP684 and UBP753 were also found to be voltage-independent; a similar degree of potentiation was observed for responses when the cells were held at either -60 mV or +20 mV (Fig. 7).

3.5 UBP684 increases NMDAR open channel probability and slows receptor deactivation time

Since UBP684 can still potentiate NMDAR responses to saturating concentrations of agonist, UBP684 appears to be increasing the receptor response in the agonist-bound state and not just simply increasing agonist potency. Thus, UBP684 is likely to be

increasing channel open probability P_{open} and/or channel conductance. To evaluate the potential effects of UBP684 on open probability, we determined the rate of block by the open channel blocker MK-801, a conventional method to estimate relative open probability (Dingledine et al., 1999). Since UBP684/753 do not show voltage-dependent activity at GluN1a/GluN2D receptors (Figure 7), they are unlikely to be interacting with MK-801 at the channel. Using GluN1a/GluN2C receptors that normally display a relatively low open probability (Dravid et al., 2008), and consequently a relatively slow rate of channel blockade (Monaghan and Larson, 1997), we found that UBP684 accelerated the rate of inhibition by 1 μM of MK-801 (control: $\tau = 3.7 \pm 0.9$ s; with UBP684: $\tau = 1.1 \pm 0.15$ s; $p = 0.02$; unpaired t-test) (Fig. 8). Similar results were found for UBP684 and UBP753 on GluN1a/GluN2D receptors (Fig. 8). In contrast, the rate of receptor blockade by the allosteric inhibitor UBP792 was unaffected by the presence of UBP684. These results suggest that UBP684 (and UBP753) increases the P_{open} of NMDARs.

A potential mechanism by which UBP684 could be enhancing NMDAR responses could be by prolonging the deactivation of the activated receptor upon agonist removal. This property could in turn change the NMDAR response to repetitive stimulation. Since GluN1a/GluN2D receptors have a remarkably slow deactivation time (Monyer et al., 1994), we were able to readily measure the effect of UBP684 and UBP753 on receptor deactivation time. In the presence of 50 μM UBP684, receptor deactivation was significantly slower as shown in Fig. 9A. The single-component, decay time following agonist removal was $\tau = 9.6 \pm 1.6$ s ($n = 11$ oocytes) in the presence of UBP684 which was significantly slower than the control (4.1 ± 0.6 s; $n = 23$ oocytes; $p <$

0.001). UBP753 did not, however, significantly change receptor deactivation time. To determine if the prolonged deactivation time was due to a slowing of steps related to L-glutamate or to glycine dissociation/inactivation, we determined the effect of UBP684 on the deactivation time associated with removing L-glutamate or glycine in the continued presence of the other agonist. Neither UBP684 nor UBP753 slowed the deactivation time induced by glycine removal in the presence of L-glutamate (Fig. 9B). However, deactivation time due to L-glutamate removal (and in the presence of glycine) was significantly slowed by UBP684 (Fig. 9C, control: τ = 9.6 ± 1.7 s, n = 6 oocytes; with UBP684 τ = 20.2 ± 4.1 s, n = 7 oocytes, p = 0.04). Consistent with the result for deactivation due to removal of both agonists, UBP753 did not slow the deactivation time for L-glutamate removal (Fig. 9C).

To determine whether the effects of UBP684 on deactivation was specific to GluN2D, which has unusually slow deactivation kinetics, or is a generalized mechanism, we also studied deactivation in the rapidly deactivating GluN1a/GluN2A receptor. To accomplish this, we expressed this receptor in HEK cells and studied the patch clamp response to rapid agonist application (< 10 ms). Rapid application of 30 μM glutamate (Glu) and 50 μM glycine (Gly) evoked macroscopic NMDAR–mediated currents that declined with a τ value of ~50 ms (Fig. 10A, black waveform). Bath application of UBP684 on its own had no effect on the HEK293 cells but enhanced NMDAR currents evoked by agonist application (Fig. 10A, red waveform). NMDAR currents peak amplitude increased two-fold (217 ± 8%, n = 4, Fig. 10B) and currents decayed much slower (356 ± 54%, n = 4, Fig. 10B), suggesting a reduction in the deactivation rate of the channels. In support of this, prolonged opening of channels was observed in isolated

outside-out patches excised from HEK293 cells in the presence of UBP684 in response to a very brief pulse of agonist. In patches with only one or a small number of channels, there was no observable change in single channel conductance. The observation that the peak response was potentiated by UBP684 during a rapid agonist pulse is consistent with experiments described above (section 3.2) suggesting that UBP684 can bind in the absence of agonist.

3.6 PAM activity requires a conformational change in the GluN2 ligand binding domain

Analysis of single channel state transitions modified by UBP684 suggest that PAM activity is associated with a reduction in long-lived shut states (unpublished observations) thought to correspond to GluN2 gating (Kussius and Popescu, 2010). This finding is consistent with the observation that UBP684 potentiation is reduced in the NMDAR construct where two opposing cysteine mutations across the cleft of the ligand binding domains (LBD) of GluN2A constrain the LBDs in the closed-cleft conformation (unpublished observations). To confirm this latter finding with UBP753, we co-expressed the disulfide crosslinked GluN1 subunit ($GluN1^C$) with wildtype GluN2A and separately co-expressed wildtype GluN1 with crosslinked GluN2A ($GluN2A^C$) and evaluated UBP753 potentiation. As previously reported (Kussius, Popescu 2010), receptors containing $GluN1^C$ were activated by L-glutamate alone and not by glycine alone, and receptors containing $GluN2A^C$ were activated by glycine and not by L-glutamate (Fig. 11). Interestingly, UBP753 potentiation was differentially affected in these mutant constructs. Compared to wildtype receptors, $GluN1^C$ containing GluN2A receptors displayed a similar level of potentiation by UBP753 whereas the $GluN2A^C$ containing receptor displayed significantly less potentiation by UBP753 (****$p<0.0001$, one way

ANOVA followed by Tukey's multiple comparison test). The potentiation of NMDAR responses by UBP753 at WT GluN2A, GluN1^{C}-containing receptors and GluN2A^{C}-containing was 51.3 ± 3.7 % (n = 17 oocytes), 39.4 ± 6.5 % (n = 9 oocytes), and 6.3 ± 1.4 % (n = 17 oocytes) respectively (Fig. 11). These results demonstrate that potentiation by UBP753 requires a conformational change in the GluN2 LBD.

4. Discussion

In the present study we have characterized the prototype NMDAR pan-PAM, UBP684 and confirmed select experiments with the structurally similar compound, UBP753. UBP684 robustly potentiates responses at native NMDARs and at all GluN1/GluN2 subtypes and displays several functional properties that make it mechanistically suitable for enhancing NMDAR activity. At GluN1/GluN2A and GluN1/GluN2B, UBP684 causes a small increase in L-glutamate and glycine agonist affinity, respectively. In addition, PAM activity is retained at all subtypes under saturating agonist conditions. Thus, they are appropriate for enhancing NMDAR responses to the mM L-glutamate levels seen in the synapse (Clements, 1996; Diamond and Jahr, 1997). These agents are also appear to be use-independent, and therefore can potentiate NMDAR responses to both phasic and tonic agonist exposures. UBP684/UBP753 activity is enhanced with lowered pH and hence would be expected to have greater potentiating activity in brain tissue of patients with schizophrenia which has a lower pH (Eastwood and Harrison, 2005; Halim et al., 2008; Lipska et al., 2006; Prabakaran et al., 2004; Torrey et al., 2005). Mechanistic studies indicate that these PAMs can increase the NMDAR open probability, and in the case of UBP684, can slow receptor deactivation time due to L-glutamate removal. Together with the observation

that conformational change at the GluN2 LBD is necessary for PAM activity, we propose that these agents stabilize the GluN2 LBD in a more active conformation.

4.1 Interactions between PAMs and agonists

Agonist concentrations can have complex effects on allosteric modulator activity. Elevated agonist concentrations can increase a modulator's potency and conversely a PAM can increase agonist potency, as seen for SGE201 (Linsenbardt et al., 2014) and GNE-8324 (Hackos et al., 2016). In such cases, saturating agonist concentrations may mask potentiating activity if the primary PAM action is to increase agonist occupation. Alternatively, high agonist concentration can increase the magnitude of the PAM's potentiation as with UBP512 (Costa et al., 2010). Increasing agonist concentration can also decrease modulator potency as seen for the GluN2C PAM PYD-106 (Khatri et al., 2014) and the NAM TCN-213 (Bettini et al., 2010). For UBP684 and UBP753, we find that potentiation of NMDAR responses remains effective at high agonist concentrations. This finding is consistent with the observation that maximal L-glutamate and glycine responses were enhanced by UBP684 and UBP753. Additionally, UBP684 caused a small increase in L-glutamate potency at GluN1/GluN2A and glycine potency at GluN1/GluN2B. Since these agents do not increase GluN1/GluN2B, GluN1/GluN2C, or GluN1/GluN2D L-glutamate potency, they should not preferentially increase extrasynaptic NMDAR currents which are exposed to lower ambient L-glutamate concentrations. Such an effect may be deleterious since extrasynaptic NMDAR activation has been associated with excitotoxicity (Hardingham and Bading, 2010). The maximal potentiation of GluN1/GluN2B responses by UBP684 was, however, reduced by approximately 40% with high agonist concentrations. This effect is consistent with the

modest increase in glycine affinity for GluN1/GluN2B receptors due to UBP684. Similarly, the neurosteroid PS causes a small increase in glycine potency and a reduction in maximal potentiation specifically at GluN1/GluN2B (Malayev et al., 2002).

Unexpectedly, UBP684 and UBP753 caused a small reduction in L-glutamate potency at GluN1/GluN2D receptors even though they are both PAMs at this receptor. Similarly, UBP684 reduced L-glutamate potency, but not glycine potency at GluN1/GluN2C receptors. Conversely, high agonist concentrations reduced UBP684 potency specifically at GluN1/GluN2D. These changes in agonist potency, however, are offset by an increase in the response magnitude, especially at higher agonist concentrations. This PAM action to reduce L-glutamate potency is potentially beneficial by reducing extrasynaptic GluN2C or GluN2D-containing receptor responses to ambient extracellular L-glutamate while still augmenting synaptic NMDAR responses. Overall, these findings indicate that UBP684/753 potentiate, partially by increasing agonist potency in a subtype-specific manner (at GluN1/GluN2A and GluN1/GluN2B receptors) and by potentiating all GluN1/GluN2 receptors by an additional mechanism which increases responses to saturating concentrations of agonist.

4.2 Use-independent PAM activity

The PAMs in this study display use-independent activity as their prior application fully potentiates subsequent agonist responses. This conclusion is also supported by experiments using rapid agonist application to receptors expressed in HEK cells (Fig. 10). Thus, UBP684 and UPB753 appear to bind to both the agonist-unbound, inactive receptor state and the agonist-bound, active state. These studies also demonstrate that UBP684/UBP753 are unlike PS which has been termed “disuse-dependent” due to a loss

of potentiating activity following agonist binding (Horak et al., 2004). A potential caveat is that UBP684/UBP753 could be slowly associating with the membrane and rapidly associating with the receptor from within the membrane. However, use-dependency was still not seen with very rapid agonist applications to HEK cells.

4.3 PAM interactions with pH

A third factor that can alter PAM activity is pH. Protons strongly inhibit NMDAR activity and can alter the function of allosteric modulators (Traynelis and Cull-Candy, 1990). For example, spermine potentiates NMDAR responses at physiologic and mild acidic conditions, but not under more alkaline conditions (Traynelis et al., 1995). Spermine causes a right-shift in the proton inhibition curve, thus spermine potentiation may be due to dis-inhibition of NMDARs inhibited by protons. Conversely, ifenprodil inhibition of NMDAR responses is associated with an increased proton sensitivity of GluN1a/GluN2B receptors (Mott et al., 1998). In the present study, we found that pH also has a strong effect on the potentiating activity of UBP684 and UBP753. Potentiation is enhanced at lower pH, and at high pH (e.g. 8.4), these PAMs display inhibitory activity. At both GluN1a/GluN2B and GluN1a/GluN2D receptors, UBP684 caused a right-shift in the proton inhibition curve. Thus, in the presence of UBP684, higher concentrations of protons are necessary to cause the same level of inhibition.

While it is possible that PAM binding partially obstructs a proton sensor, PAM binding may be simply promoting receptor conformations that over-ride the negative modulation by protons. Amino acid residues in the M3, the M3-S2 linker, and the S2-M4 linker mediate proton inhibition of NMDARs (Low et al., 2003) and these regions are closely associated with channel gating as modulated by the N-terminal and S1/S2

domains. Thus, PAM binding in the S1/S2, or in the linker regions, may allosterically counter the inhibitory effects of protons near the channel gate. Conversely, at a proton-uninhibited alkaline pH, the coupling of agonist and channel-gating may be sufficiently optimal that PAM binding can not further increase coupling. The inhibitory activity of UBP684, UBP753, and GNE-8324 under alkaline conditions suggests the possibility that PAM binding may be stabilizing conformations intermediate between the proton-inhibited and proton-uninhibited states thus making UBP684/UBP753 binding inhibitory at pH 8.4. Alternatively, inhibitory activity could result from UBP684 and UBP753 binding to a second site that is inhibitory whose activity is revealed at alkaline pH. Neurosteroids and compounds structurally-related to UBP684/UBP753 display both NAM and PAM activity at distinct sites and often display greater inhibitory activity at GluN2C and GluN2D as seen here (Costa et al., 2010; Horak et al., 2006; Irvine et al., 2012; Malayev et al., 2002).

UBP684 has an additional effect at GluN1a/GluN2D receptors wherein increasing proton concentration from pH 8.5 to pH 7.5 leads to a 3-fold increase in receptor response. Then, further increases in H^+ concentration (pH 7.5 to pH 5.5) decrease the response in accord with proton inhibition. The UBP684-potentiated GluN1/GluN2D response at pH 7.5 is significantly larger (~50%) than the response in the absence of UBP684 at pH 8.5 where there is little proton inhibition (Traynelis and Cull-Candy, 1990). Thus, unlike spermine, UBP684 potentiates more than what can be accounted for by reversal of proton inhibition. Another distinction between UPB684 and spermine is that spermine potentiation is mostly prevented by the presence of the N-terminal insert of GluN1b whereas UBP684 potentiation is unaffected.

Greater PAM activity under more acidic conditions has potential therapeutic implications. In the brain from patients with schizophrenia, there is a nearly 0.2 decrease in pH (Eastwood and Harrison, 2005; Halim et al., 2008; Lipska et al., 2006; Prabakaran et al., 2004; Torrey et al., 2005). Thus, NMDAR hypofunction should be worsened in schizophrenia and a PAM that shows increased activity under more acidic conditions should show greater effects in patients with schizophrenia than in healthy subjects.

4.4 PAM mechanism of action

UBP684 and UBP753 accelerate the rate of MK-801 inhibition. As an open channel blocker, MK-801's rate of blockade is proportional to the channel open probability (Dingledine et al., 1999). Thus, the acceleration of MK-801 blockade by UBP684 or UBP753 suggests that the PAM increases open channel probability. Furthermore, UBP684 had no effect on GluN1/GluN2A channel conductance. Thus, together with the observations that UBP684/UBP753 can potentiate without increasing agonist potency, these observations support the idea that these agents potentiate by increasing open probability. Precisely which gating steps account for the increased open probability remains to be determined.

The modulation of the receptor deactivation rate also contributes to UBP684 PAM activity. In the presence of UBP684, GluN1/GluN2A and GluN1/GluN2D deactivation rate is slowed following L-glutamate removal. Thus, the PAM appears to either slow L-glutamate dissociation and/or slow a channel-gating deactivation step after L-glutamate dissociation. If there were only a slowing of L-glutamate dissociation, one would expect that UBP684 would increase L-glutamate potency at GluN1/GluN2A and GluN1/GluN2D receptors. There is an increase in potency at GluN2A, but a decrease at

GluN1/GluN2D receptors. Thus, at GluN2D-containing receptors, there may be some other compensation such as a decrease in the L-glutamate association rate. Similarly, at GluN1/GluN2C, the PAM CIQ also slows receptor deactivation without increasing agonist potency (Mullasseril et al., 2010).

Slowing of GluN1/GluN2A deactivation was also seen in separate experiments in the dialyzed, whole-cell recording mode in which steady-state potentiation of GluN1/GluN2A responses by UBP684 are eliminated (unpublished observations). Thus, the effects of UBP684 on steady-state potentiation and receptor deactivation appears to have at least partially distinct mechanisms.

Interestingly, the ability to modulate receptor deactivation differs significantly between PAMs, even for those with closely related structures. We find that unlike UBP684, UBP753 does not slow the GluN1/GluN2D deactivation time upon L-glutamate removal. Similarly, GNE-8324, but not the related PAM GNE-6901, slows the L-glutamate deactivation rate (Hackos and Hanson, 2017). Of other PAMs, PS slows the deactivation rate (Ceccon et al., 2001), CIQ does not (Mullasseril et al., 2010), and PYD-106 accelerates the deactivation rate even though it is a PAM (Khatri et al., 2014). These differences are expected to have functional implications; PAMs that slow deactivation may increase summation of synaptic responses during a stimulus train of the appropriate frequency.

UBP753 potentiation requires conformational flexibility at GluN2A but not at GluN1 subunits. Thus, locking the GluN2 LBD in the closed, active conformation by disulfide bonds appears to obscure PAM activity, suggesting that the PAM stabilizes the glutamate-bound conformation or associated channel-gating conformations. This result is

consistent with that found for UBP684 potentiation of NMDAR responses and with analysis of single channel state transitions as modified by UBP684 (unpublished observations). Thus, PAM activity may stabilize the glutamate-bound conformation and thereby slow glutamate dissociation, but only UBP684, and not UBP753, slowed deactivation upon glutamate removal. A potential caveat for these studies is that the GluN2 locked-LBD receptor may have a maximal open probability, thereby obscuring further potentiation. However, this construct is potentiated by a similar amount as are wildtype receptors when potentiated by a biochemical method which maximizes open probability (Blanke and VanDongen, 2008).

While more work is necessary to fully define the binding site(s) for UBP684/UBP753, what is currently known is consistent with an action at the GluN2 LBD/LBD-TM linker region which could account for the physiological properties describe above. Our prior studies with the structurally-related PAMs, UBP512 (GluN2A-selective) and UBP710 (GluN2A/B-selective) were able to use their subtype selectivity and GluN2A/GluN2C chimeras to show that their activity is associated with the S2 segment of the GluN2 LBD. Also, their PAM activity is not eliminated by deletion of both the GluN1 and GluN2 N-terminals. Thus, these agents do not appear to be acting at the N-terminal binding site as found for spermine (Paoletti and Neyton, 2007; Traynelis et al., 1995) nor at the LBD/N-terminal interface at which PYD-106 is thought to bind (Khatri et al., 2014). They also do not appear to bind at the pre-M1/M1 site proposed for CIQ (Mullasseril et al., 2010) and do not compete for agonist binding within the LBD (Costa et al., 2010). The involvement of the S2 domain, suggests that these agents may be binding at the LBD dimer interface as recently shown for GNE-6901 (Hackos et al.,

2016). They could also possibly be binding at the overlapping S2 /S2-TM linker as proposed for neurosteroids (Kostakis et al., 2011). Potentially, either of these locations could account for the stabilization of the L-glutamate-bound open channel receptor conformation as suggested by the present results.

5. General conclusions

The alkyl-naphthoic acid PAMs characterized here add to the pharmacodynamic diversity of the rapidly expanding list of NMDAR PAMs such as PS (Chopra et al., 2015; Horak et al., 2006; Horak et al., 2004; Jang et al., 2004; Kostakis et al., 2011; Wu et al., 1991), UBP512, UBP646 (Costa et al., 2010), UBP714 (Irvine et al., 2012), CIQ (Mullasseril et al., 2010), PYD106 (Khatri et al., 2014), SGE201 (Linsenbardt et al., 2014; Paul et al., 2013), and GNE6901 (Hackos et al., 2016). These agents differ in their subtype-selectivity, N-terminal insert-sensitivity, pH-sensitivity, use/disuse-dependency, and their effects on agonist potency, efficacy and deactivation. They also differ in how their modulatory activity is affected by different agonist concentrations. These varied properties means that it is possible to pharmacologically target distinct NMDAR populations in specific physiological conditions. Thus, there is significant potential to develop NMDAR PAMs with optimal properties for cognitive enhancement and for improving function in conditions of NMDAR hypofunction such as schizophrenia.

Acknowledgements

This work was supported by the National Institutes of Mental Health (Grant MH60252) and the UK Medical Research Council (G0601509, G0601812) and the BBSRC (grant BB/L001977/1). We gratefully acknowledge Drs. Shigetada Nakanishi, Peter Seeburg,

Dolan Pritchett David Lynch, and Gabriela Popescu for providing cDNA constructs used in this study.

Abbreviations

AMPA, 2-amino-3-hydroxy-5-methyl-4-isoxazole propionic acid

CIQ, 3-chlorophenyl (6,7-dimethoxy-1-((4-methoxyphenoxy)methyl)-3,4-dihydroisoquinolin-2(1H)-yl) methanone

DTPA, diethylenetriaminepentaacetic acid

HEPES, 4-(2-hydroxyethyl)-1-piperazineethanesulfonic acid

LBD, ligand binding domain

M1, NMDAR 1st membrane-associated segment

NAM, negative allosteric modulator

NMDAR, N-methyl-D-aspartate receptor

PAM, positive allosteric modulator

PS, pregnenalone sulphate

S2, segment 2 of the NMDAR LBD

TM, transmembrane segment of the NMDAR

References:

Bettini, E., Sava, A., Griffante, C., Carignani, C., Buson, A., Capelli, A. M., Negri, M., Andreetta, F., Senar-Sancho, S. A., Guiral, L., Cardullo, F., 2010. Identification and characterisation of novel NMDA receptor antagonists selective for NR2A- over NR2B-containing receptors. J Pharmacol Exp Ther 335, 636-644.

Blanke, M. L., VanDongen, A. M., 2008. Constitutive activation of the N-methyl-D-aspartate receptor via cleft-spanning disulfide bonds. J Biol Chem 283, 21519-21529.

Bresink, I., Benke, T. A., Collett, V. J., Seal, A. J., Parsons, C. G., Henley, J. M., Collingridge, G. L., 1996. Effects of memantine on recombinant rat NMDA receptors expressed in HEK 293 cells. Br J Pharmacol 119, 195-204.

Buller, A. L., Larson, H. C., Schneider, B. E., Beaton, J. A., Morrisett, R. A., Monaghan, D. T., 1994. The molecular basis of NMDA receptor subtypes: native receptor diversity is predicted by subunit composition. J Neurosci 14, 5471-5484.

Ceccon, M., Rumbaugh, G., Vicini, S., 2001. Distinct effect of pregnenolone sulfate on NMDA receptor subtypes. Neuropharmacology 40, 491-500.

Chesler, M., Kaila, K., 1992. Modulation of pH by neuronal activity. Trends Neurosci 15, 396-402.

Chopra, D. A., Monaghan, D. T., Dravid, S. M., 2015. Bidirectional Effect of Pregnenolone Sulfate on GluN1/GluN2A N-Methyl-D-Aspartate Receptor Gating Depending on Extracellular Calcium and Intracellular Milieu. Mol Pharmacol 88, 650-659.

Clements, J. D., 1996. Transmitter timecourse in the synaptic cleft: its role in central synaptic function. Trends Neurosci 19, 163-171.

Costa, B. M., Irvine, M. W., Fang, G., Eaves, R. J., Mayo-Martin, M. B., Laube, B., Jane, D. E., Monaghan, D. T., 2012. Structure-activity relationships for allosteric NMDA receptor inhibitors based on 2-naphthoic acid. Neuropharmacology 62, 1730-1736.

Costa, B. M., Irvine, M. W., Fang, G., Eaves, R. J., Mayo-Martin, M. B., Skifter, D. A., Jane, D. E., Monaghan, D. T., 2010. A novel family of negative and positive allosteric modulators of NMDA receptors. J Pharmacol Exp Ther 335, 614-621.

Coyle, J. T., 2006. Glutamate and schizophrenia: beyond the dopamine hypothesis. Cell Mol Neurobiol 26, 365-384.

Diamond, J. S., Jahr, C. E., 1997. Transporters buffer synaptically released glutamate on a submillisecond time scale. J Neurosci 17, 4672-4687.

Dingledine, R., Borges, K., Bowie, D., Traynelis, S. F., 1999. The glutamate receptor ion channels. Pharmacol Rev 51, 7-61.

Dravid, S. M., Prakash, A., Traynelis, S. F., 2008. Activation of recombinant NR1/NR2C NMDA receptors. J Physiol 586, 4425-4439.

Eastwood, S. L., Harrison, P. J., 2005. Decreased expression of vesicular glutamate transporter 1 and complexin II mRNAs in schizophrenia: further evidence for a synaptic pathology affecting glutamate neurons. Schizophr Res 73, 159-172.

Greenwood, T. A., Light, G. A., Swerdlow, N. R., Radant, A. D., Braff, D. L., 2012. Association analysis of 94 candidate genes and schizophrenia-related endophenotypes. PLoS One 7, e29630.

Hackos, D. H., Hanson, J. E., 2017. Diverse modes of NMDA receptor positive allosteric modulation: Mechanisms and consequences. Neuropharmacology 112, 34-45.

Hackos, D. H., Lupardus, P. J., Grand, T., Chen, Y., Wang, T. M., Reynen, P., Gustafson, A., Wallweber, H. J., Volgraf, M., Sellers, B. D., Schwarz, J. B., Paoletti, P., Sheng, M., Zhou, Q., Hanson, J. E., 2016. Positive Allosteric Modulators of GluN2A-Containing NMDARs with Distinct Modes of Action and Impacts on Circuit Function. Neuron 89, 983-999.

Halim, N. D., Lipska, B. K., Hyde, T. M., Deep-Soboslay, A., Saylor, E. M., Herman, M. M., Thakar, J., Verma, A., Kleinman, J. E., 2008. Increased lactate levels and reduced pH in

postmortem brains of schizophrenics: medication confounds. J Neurosci Methods 169, 208-213.

Hardingham, G. E., Bading, H., 2010. Synaptic versus extrasynaptic NMDA receptor signalling: implications for neurodegenerative disorders. Nat Rev Neurosci 11, 682-696.

Hollmann, M., Boulter, J., Maron, C., Beasley, L., Sullivan, J., Pecht, G., Heinemann, S., 1993. Zinc potentiates agonist-induced currents at certain splice variants of the NMDA receptor. Neuron 10, 943-954.

Horak, M., Vlcek, K., Chodounska, H., Vyklicky, L., Jr., 2006. Subtype-dependence of N-methyl-D-aspartate receptor modulation by pregnenolone sulfate. Neuroscience 137, 93-102.

Horak, M., Vlcek, K., Petrovic, M., Chodounska, H., Vyklicky, L., Jr., 2004. Molecular mechanism of pregnenolone sulfate action at NR1/NR2B receptors. J Neurosci 24, 10318-10325.

Ikeda, K., Nagasawa, M., Mori, H., Araki, K., Sakimura, K., Watanabe, M., Inoue, Y., Mishina, M., 1992. Cloning and expression of the epsilon 4 subunit of the NMDA receptor channel. FEBS Lett 313, 34-38 availability.

Irvine, M. W., Costa, B. M., Volianskis, A., Fang, G., Ceolin, L., Collingridge, G. L., Monaghan, D. T., Jane, D. E., 2012. Coumarin-3-carboxylic acid derivatives as potentiators and inhibitors of recombinant and native N-methyl-d-aspartate receptors. Neurochem Int.

Irvine, M. W., Fang, G., Eaves, R., Mayo-Martin, M. B., Burnell, E. S., Costa, B. M., Culley, G. R., Volianskis, A., Collingridge, G. L., Monaghan, D. T., Jane, D. E., 2015. Synthesis of a Series of Novel 3,9-Disubstituted Phenanthrenes as Analogues of Known NMDA Receptor Allosteric Modulators. Synthesis (Stuttg) 47, 1593-1610.

Ishii, T., Moriyoshi, K., Sugihara, H., Sakurada, K., Kadotani, H., Yokoi, M., Akazawa, C., Shigemoto, R., Mizuno, N., Masu, M., al., e., 1993. Molecular characterization of the family of the N-methyl-D-aspartate receptor subunits. J Biol Chem 268, 2836-2843.

Jang, M. K., Mierke, D. F., Russek, S. J., Farb, D. H., 2004. A steroid modulatory domain on NR2B controls N-methyl-D-aspartate receptor proton sensitivity. Proc Natl Acad Sci U S A 101, 8198-8203.

Kamat, P. K., Kalani, A., Rai, S., Swarnkar, S., Tota, S., Nath, C., Tyagi, N., 2016. Mechanism of Oxidative Stress and Synapse Dysfunction in the Pathogenesis of Alzheimer's Disease: Understanding the Therapeutics Strategies. Mol Neurobiol 53, 648-661.

Kantrowitz, J. T., Javitt, D. C., 2010. Thinking glutamatergically: changing concepts of schizophrenia based upon changing neurochemical models. Clin Schizophr Relat Psychoses 4, 189-200.

Khatri, A., Burger, P. B., Swanger, S. A., Hansen, K. B., Zimmerman, S., Karakas, E., Liotta, D. C., Furukawa, H., Snyder, J. P., Traynelis, S. F., 2014. Structural determinants and mechanism of action of a GluN2C-selective NMDA receptor positive allosteric modulator. Mol Pharmacol 86, 548-560.

Kohr, G., Eckardt, S., Luddens, H., Monyer, H., Seeburg, P. H., 1994. NMDA receptor channels: subunit-specific potentiation by reducing agents. Neuron 12, 1031-1040 availability.

Kostakis, E., Jang, M. K., Russek, S. J., Gibbs, T. T., Farb, D. H., 2011. A steroid modulatory domain in NR2A collaborates with NR1 exon-5 to control NMDAR modulation by pregnenolone sulfate and protons. J Neurochem 119, 486-496.

Koutsilieri, E., Riederer, P., 2007. Excitotoxicity and new antiglutamatergic strategies in Parkinson's disease and Alzheimer's disease. Parkinsonism Relat Disord 13 Suppl 3, S329-331.

Kussius, C. L., Popescu, G. K., 2010. NMDA receptors with locked glutamate-binding clefts open with high efficacy. J Neurosci 30, 12474-12479.

Linsenbardt, A. J., Taylor, A., Emnett, C. M., Doherty, J. J., Krishnan, K., Covey, D. F., Paul, S. M., Zorumski, C. F., Mennerick, S., 2014. Different oxysterols have opposing actions at N-methyl-D-aspartate receptors. Neuropharmacology 85, 232-242.

Lipska, B. K., Deep-Soboslay, A., Weickert, C. S., Hyde, T. M., Martin, C. E., Herman, M. M., Kleinman, J. E., 2006. Critical factors in gene expression in postmortem human brain: Focus on studies in schizophrenia. Biol Psychiatry 60, 650-658.

Lisman, J. E., Coyle, J. T., Green, R. W., Javitt, D. C., Benes, F. M., Heckers, S., Grace, A. A., 2008. Circuit-based framework for understanding neurotransmitter and risk gene interactions in schizophrenia. Trends Neurosci 31, 234-242.

Low, C. M., Lyuboslavsky, P., French, A., Le, P., Wyatte, K., Thiel, W. H., Marchan, E. M., Igarashi, K., Kashiwagi, K., Gernert, K., Williams, K., Traynelis, S. F., Zheng, F., 2003. Molecular determinants of proton-sensitive N-methyl-D-aspartate receptor gating. Mol Pharmacol 63, 1212-1222.

Luykx, J. J., Bakker, S. C., Visser, W. F., Verhoeven-Duif, N., Buizer-Voskamp, J. E., den Heijer, J. M., Boks, M. P., Sul, J. H., Eskin, E., Ori, A. P., Cantor, R. M., Vorstman, J., Strengman, E., DeYoung, J., Kappen, T. H., Pariama, E., van Dongen, E. P., Borgdorff, P., Bruins, P., de Koning, T. J., Kahn, R. S., Ophoff, R. A., 2015. Genome-wide association study of NMDA receptor coagonists in human cerebrospinal fluid and plasma. Mol Psychiatry 20, 1557-1564.

Malayev, A., Gibbs, T. T., Farb, D. H., 2002. Inhibition of the NMDA response by pregnenolone sulphate reveals subtype selective modulation of NMDA receptors by sulphated steroids. Br J Pharmacol 135, 901-909.

Mishina, M., Mori, H., Araki, K., Kushiya, E., Meguro, H., Kutsuwada, T., Kashiwabuchi, N., Ikeda, K., Nagasawa, M., Yamazaki, M., et al., 1993. Molecular and functional diversity of the NMDA receptor channel. Ann N Y Acad Sci 707, 136-152.

Monaghan, D. T., Bridges, R. J., Cotman, C. W., 1989. The excitatory amino acid receptors: their classes, pharmacology, and distinct properties in the function of the central nervous system. Annu Rev Pharmacol Toxicol 29, 365-402.

Monaghan, D. T., Larson, H., 1997. NR1 and NR2 subunit contributions to N-methyl-D-aspartate receptor channel blocker pharmacology. J Pharmacol Exp Ther 280, 614-620.

Monyer, H., Burnashev, N., Laurie, D. J., Sakmann, B., Seeburg, P. H., 1994. Developmental and regional expression in the rat brain and functional properties of four NMDA receptors. Neuron 12, 529-540.

Mott, D. D., Doherty, J. J., Zhang, S., Washburn, M. S., Fendley, M. J., Lyuboslavsky, P., Traynelis, S. F., Dingledine, R., 1998. Phenylethanolamines inhibit NMDA receptors by enhancing proton inhibition. Nat Neurosci 1, 659-667.

Mullasseril, P., Hansen, K. B., Vance, K. M., Ogden, K. K., Yuan, H., Kurtkaya, N. L., Santangelo, R., Orr, A. G., Le, P., Vellano, K. M., Liotta, D. C., Traynelis, S. F., 2010. A subunit-selective potentiator of NR2C- and NR2D-containing NMDA receptors. Nat Commun 1, 1-8.

Paoletti, P., Neyton, J., 2007. NMDA receptor subunits: function and pharmacology. Curr Opin Pharmacol 7, 39-47.

Paul, S. M., Doherty, J. J., Robichaud, A. J., Belfort, G. M., Chow, B. Y., Hammond, R. S., Crawford, D. C., Linsenbardt, A. J., Shu, H. J., Izumi, Y., Mennerick, S. J., Zorumski, C. F., 2013. The major brain cholesterol metabolite 24(S)-hydroxycholesterol is a potent allosteric modulator of N-methyl-D-aspartate receptors. J Neurosci 33, 17290-17300.

Pivovarova, N. B., Andrews, S. B., 2010. Calcium-dependent mitochondrial function and dysfunction in neurons. FEBS J 277, 3622-3636.

Prabakaran, S., Swatton, J. E., Ryan, M. M., Huffaker, S. J., Huang, J. T., Griffin, J. L., Wayland, M., Freeman, T., Dudbridge, F., Lilley, K. S., Karp, N. A., Hester, S., Tkachev, D., Mimmack, M. L., Yolken, R. H., Webster, M. J., Torrey, E. F., Bahn, S., 2004. Mitochondrial dysfunction in schizophrenia: evidence for compromised brain metabolism and oxidative stress. Mol Psychiatry 9, 684-697, 643.

Schizophrenia Working Group of the Psychiatric Genomics, C., 2014. Biological insights from 108 schizophrenia-associated genetic loci. Nature 511, 421-427.

Siesjo, B. K., 1985. Acid-base homeostasis in the brain: physiology, chemistry, and neurochemical pathology. Prog Brain Res 63, 121-154.

Sugihara, H., Moriyoshi, K., Ishii, T., Masu, M., Nakanishi, S., 1992. Structures and properties of seven isoforms of the NMDA receptor generated by alternative splicing. Biochem Biophys Res Commun 185, 826-832.

Sullivan, J. M., Traynelis, S. F., Chen, H. S., Escobar, W., Heinemann, S. F., Lipton, S. A., 1994. Identification of two cysteine residues that are required for redox modulation of the NMDA subtype of glutamate receptor. Neuron 13, 929-936.

Sun, J., Jia, P., Fanous, A. H., van den Oord, E., Chen, X., Riley, B. P., Amdur, R. L., Kendler, K. S., Zhao, Z., 2010. Schizophrenia gene networks and pathways and their applications for novel candidate gene selection. PLoS One 5, e11351.

Torrey, E. F., Barci, B. M., Webster, M. J., Bartko, J. J., Meador-Woodruff, J. H., Knable, M. B., 2005. Neurochemical markers for schizophrenia, bipolar disorder, and major depression in postmortem brains. Biol Psychiatry 57, 252-260.

Traynelis, S. F., Cull-Candy, S. G., 1990. Proton inhibition of N-methyl-D-aspartate receptors in cerebellar neurons. Nature 345, 347-350.

Traynelis, S. F., Hartley, M., Heinemann, S. F., 1995. Control of proton sensitivity of the NMDA receptor by RNA splicing and polyamines. Science 268, 873-876.

Vicini, S., Wang, J. F., Li, J. H., Zhu, W. J., Wang, Y. H., Luo, J. H., Wolfe, B. B., Grayson, D. R., 1998. Functional and pharmacological differences between recombinant N-methyl- D-aspartate receptors. J Neurophysiol 79, 555-566.

Watanabe, M., Inoue, Y., Sakimura, K., Mishina, M., 1992. Developmental changes in distribution of NMDA receptor channel subunit mRNAs. Neuroreport 3, 1138-1140.

Watanabe, M., Inoue, Y., Sakimura, K., Mishina, M., 1993. Distinct distributions of five N-methyl-D-aspartate receptor channel subunit mRNAs in the forebrain. J Comp Neurol 338, 377-390.

Watkins, J. C., Evans, R. H., 1981. Excitatory amino acid transmitters. Annu Rev Pharmacol Toxicol 21, 165-204.

Watkins, J. C., Krogsgaard Larsen, P., Honore, T., 1990. Structure-activity relationships in the development of excitatory amino acid receptor agonists and competitive antagonists. Trends Pharmacol Sci 11, 25-33.

Wu, F. S., Gibbs, T. T., Farb, D. H., 1991. Pregnenolone sulfate: a positive allosteric modulator at the N-methyl-D-aspartate receptor. Mol Pharmacol 40, 333-336.

Table 1 Potentiation by UBP684 and UBP753 of GluN1/GluN2 NMDAR responses

Compound	Glu/Gly.	GluN2A	GluN2B	GluN2C	GluN2D
UBP684	10 µM / 10 µM	28.0 ± 4.6 (68.6 ± 16.2)	34.6 ± 3 (102.0 ± 17.8)$^{###}$	37.2 ± 2.8 (117.2 ± 22.3)	28.9 ± 4.1 (88.4 ± 9.6)
UBP684	300 µM / 300 µM	10.3 ± 4.8* (50.3 ± 14.1)	24.8 ± 2.8* (61.5 ± 4.2)	33.8 ± 9.7 (108.2 ± 37.9)	55.8 ± 4.1** (119.3 ± 37.9)
UBP753	10 µM / 10 µM	39.4 ± 27.5 (277.2 ± 36.8)	25.0 ± 11.6 (192.3 ± 46.6)	36.2± 5.7 (262.6 ± 33.9)	30.6 ± 7.5 (240.3 ± 63.6)

EC_{50} values (mean ± S.E.M.) for PAM potentiation of GluN1/GluN2 NMDAR responses. Values in parenthesis represent the maximal potentiation (% E_{Max}) expressed as a percentage (± S.E.M.) above the agonist-alone response (10 µM L-glutamate and 10 µM glycine).

$^{*}p < 0.05$ and $^{**}p < 0.01$ (unpaired t-test) vs EC_{50} value for UBP684 potentiation at 10 µM L-glutamate and 10 µM glycine.

$^{###}p < 0.001$ (unpaired t-test) vs % E_{Max} value for UBP684 potentiation at 10 µM L-glutamate and 10 µM glycine.

Table 2 The effect of UBP684 and UBP753 on the potency and maximal effect of L-glutamate and glycine at NMDAR containing different GluN2 subunits.

		Glutamate		
		EC_{50} (μM)	*% Control $_{Max}$*	*N*
GluN2A	- UBP684	4.62 ± 0.32	99.0 ± 1.25	12
	+ UBP684	3.12 ± 0.52*	120.4 ± 4.5	12
GluN2B	- UBP684	2.01 ± 0.19	104.6 ± 1.8	9
	+ UBP684	2.08 ± 0.12	152.3 ± 6.3	7
GluN2C	- UBP684	1.32 ± 0.1	96.7 ± 2.0	16
	+ UBP684	2.09 ± 0.18**	136.5 ± 3.1	13
GluN2D	- UBP684	0.88 ± 0.05	99.6 ± 1.2	10
	+ UBP684	1.4 ± 0.1***	141.1 ± 5.5	7
GluN2D	- UBP753	0.93 ± 0.06	100.7 ± 1.6	15
	+ UBP753	1.3 ± 0.1**	128.3 ± 3.8	6
		Glycine		
		EC_{50} (μM)	*% Control $_{Max}$*	*N*
GluN2A	- UBP684	0.42 ± 0.05	98.3 ± 2.2	9
	+ UBP684	0.46 ± 0.03	124.5 ± 2.3	8
GluN2B	- UBP684	0.87 ± 0.07	101.9 ± 2.7	19
	+ UBP684	0.61 ± 0.05**	119.4 ± 3.0	19
GluN2C	- UBP684	0.68 ± 0.08	99.6 ± 2.1	9
	+ UBP684	0.72 ± 0.04	137.2 ± 1.8	12
GluN2D	- UBP684	0.32 ± 0.04	97.0 ± 2.6	9
	+ UBP684	0.25 ± 0.01	131.0 ± 2.9	6
GluN2D	- UBP753	0.2 ± 0.04	96.5 ± 2.9	14
	+ UBP753	0.22 ± 0.03	135.4 ± 3.8	7

EC_{50} values (mean ± S.E.M.) and maximal response size for PAM potentiation of GluN1/GluN2 NMDAR responses. $^{*}p < 0.05$, $^{**}p < 0.01$ and $^{***}p < 0.001$ for differences between agonist EC_{50} values without UBP684 (or UBP753) at the same NMDAR subtype. *% Control $_{Max}$* is the maximal response as a % of the maximal control response in the absence of the PAM. *N* = number of experiments.

Figure Legends

Figure 1.

Potentiation of GluN2A-D and native NMDARs by UBP684.

(**A**) Chemical structures of UBP684 and UBP753. (**B**) Representative current traces showing UBP684 (100 μM, gray bar) enhancement of GluN1a/GluN2A-D receptor-mediated currents evoked by 10 μM L-glutamate and 10 μM glycine (black bar). Scale: X-axis = 17 s, 10 s, 10 s, and 17 s and y-axis = 60 nA, 115 nA, 75 nA and 85 nA for GluN1/GluN2A, GluN1/GluN2B, GluN1/GluN2C, and GluN1/GluN2D traces respectively. (**C**) Dose-response for UBP684 potentiation of currents evoked by low (left panel) agonist concentrations (10 μM L-glutamate and 10 μM glycine, left panel) and high (right panel) agonist concentrations (300 μM L-glutamate and 300 μM glycine) at NMDARs containing GluN2A (red), GluN2B (green), GluN2C (blue), or GluN2D (gray) subunits. Values represent mean ± SEM % potentiation over the agonist-alone response. N = 5 - 12 oocytes per subunit. (**D**) Whole-cell recordings of CA1 pyramidal cell NMDAR responses to picospritzer pulse applications of 100 μM NMDA plus 100 μM glycine in the absence (control), presence of 60 μM UBP684 in the bath, or after UBP684 washout. The potentiation by UBP684 (60 μM) of NMDAR currents was reversed upon UBP684 washout (wash) and the NMDAR currents were blocked by 100 μM DL-AP5. Histogram (right) shows the mean ± S.E.M. potentiation relative to the initial agonist peak response for bath applied UBP684 and following washout. * significantly different from 0 % potentiation and from the wash condition ($n = 5$, $p < 0.05$).

Figure 2.

Effect of UBP684 on L-glutamate and glycine potency and maximal response.

Concentration-response for L-glutamate (left panel) and glycine (right panel) excitation of GluN2A- (**A**), GluN2B- (**B**), GluN2C- (**C**) and GluN2D- (**D**) containing NMDARs in the absence (black) or presence (red, GluN2A; green, GluN2B; blue, GluN2C; and gray, GluN2D) of 50 μM UBP684. In each experiment, the co-agonist (L-glutamate or glycine) was used at 10 μM. The responses from each oocyte were individually normalized with the response obtained from the highest concentration of the agonist-alone application in the same oocyte. Data represent mean ± S.E.M., n = 6 - 19 oocytes.

Figure 3.

UBP753 potentiation of NMDAR activity and its effect on agonist affinity.

(**A**) UBP753 concentration-response for the potentiation of NMDAR-mediated current induced by 10 μM of L-glutamate and 10 μM glycine and expressed as % potentiation of agonist-alone induced responses (n = 5-12 oocytes). (**B**) Single exponential fits the onset (τ_{on}) and offset (τ_{off}) for UBP753 potentiation of GluN2D-containing NMDARs at different concentrations of UBP753 were plotted as $1/\tau$ as a function of UBP753 concentration. Rates were determined by single-exponential fit of the onset-rates and offset-rates. As expected, onset was concentration-dependent and off-set was concentration independent. On-rate and off-rate was used to calculate K_d as described in the text. L-glutamate (**C**) or glycine (**D**) dose-response in the absence (black) or presence (red) of 30 μM UBP753 at GluN2D-containing NMDARs (n = 6 - 15 oocytes per curve). Co-agonist was present at 10 μM in both C and D. Data represent mean ± S.E.M.

Figure 4.

UBP684/753 bind to both agonist-bound and agonist-unbound states of NMDARs.

(**A**) UBP753 (top panel) and UBP684 (bottom panel) potentiation of agonist-evoked GluN1/GluN2B responses in five different drug-application protocols - left to right: agonist alone, sequential, co-application, pre-co application, and cotemporaneous. Drugs were applied as indicated by bars above the responses (black, 10 μM L-glutamate and 10 μM glycine), UBP753 (red, 100 μM) and UBP684 (green, 50 μM). Scale bar: horizontal = time in sec, vertical = current in nA. (**B**) Average agonist response onset rates (τ_w, weighted fit) for the different application protocols for UBP684, except for cotemporaneous which represents the onset of UBP684 potentiation. (**C**) Magnitude of UBP684 potentiation in the different drug application paradigms. Data represent mean ± SEM, **p<0.01, ***p<0.001, ****p<0.0001 (one-way ANOVA followed by Tukey's multiple comparison test, n = 8 oocytes).

Figure 5.

Effect of extracellular pH on the modulation of NMDAR activity by UBP684.

(A) Representative current traces showing the effect of extracellular pH (7.4 and 8.4) on UBP684 activity at recombinant GluN1/GluN2A-D receptors. During a steady-state response evoked by 10 μM L-glutamate / 10 μM glycine (black bar), UBP684 (100 μM, green bar) was co-applied with the agonists. UBP684 potentiated NMDAR responses at pH 7.4 (left trace, see also Fig. 1A) and inhibited all responses at pH 8.4 (4 traces on right). (**B)** Percent response potentiation by UBP684 (100 μM) at the 4 GluN1a/GluN2 receptors at pH 7.4 (blue) and pH 8.4 (red). Values represent mean ± SEM, n = 6 - 9 oocytes. Inhibition is reflected by negative % potentiation values. **(C)** UBP753 (50 μM) modulation of GluN1a/GluN2C receptors at pH 6.4, 7.4, and 8.4, n = 14 or more oocytes).

(**D**) Pregnenolone sulfate (PS, 100 μM) potentiation of GluN1a/GluN2A and GluN1a/GluN2B receptor responses evoked by 10 μM L-glutamate / 10 μM glycine at pH 7.4 (blue) and pH 8.4 (red), n = 8 oocytes. (**E**) Effect of pH on potentiation of GluN1a/GluN2C NMDAR responses by 30 μM CIQ, a GluN2C/GluN2D-selective PAM, n = 11 oocytes. (**F**) Effect of pH on 30 μM GNE-8324 potentiation of GluN1a/GluN2A receptor responses. Inhibition is reflected by negative % potentiation values, n = 15 oocytes. Data represent mean ± SEM, *p<0.05, **p<0.01, ****p<0.0001.

Figure 6.

UBP684 interaction with protons and the N-terminal GluN1 insert.

Proton inhibition of GluN2B- (**A**) and GluN2D- (**B**) containing NMDARs was determined in the absence (black) or presence (green) of 50 μM UBP684. Responses from each oocyte were normalized to the NMDAR response obtained at pH 8.5 in absence of UBP684 from the same oocyte, n = 8 - 12 oocytes. (**C**) UBP684 potentiation of GluN1a/GluN2D (blue, solid curve) and GluN1b/GluN2D (blue, dotted curve) receptors at pH 7.4. Values represent the % potentiation above the agonist-alone control response, n = 5 - 6 oocytes. (**D**) UBP684 inhibition of GluN1a/GluN2D (red, solid curve) and GluN1b/GluN2D (red, dotted curve) receptors at pH 8.4, n = 5 - 7 oocytes. Values represent the mean ± SEM % inhibition.

Figure 7.

Effect of redox modulation and membrane potential on PAM activity.

(**A**) Average % potentiation by UBP684 (50 μM, green bars) and UBP753 (50 μM, red bars) before (open bars) and after (solid bars) 3 mM DTT treatment of GluN2D-containing NMDARs for 3 min (n = 8 oocytes). (**B**) Top: represented traces showing the potentiation by UBP684 and

UBP753 when membrane potential was held at + 20 mV (gray) or at – 60 mV (black). Bottom: Histogram showing average potentiation by UBP 684 (50 μM, green bars) and UBP753 (50 μM, red bars) at GluN1/GluN2C receptors when the membrane potential was held at + 20 mV or at – 60 mV (n = 4 oocytes). Data represent mean ± SEM.

Figure 8.

Effect of UBP684 and UBP753 on the rate of MK-801 channel blockade as a measure of open channel probability.

(**A**) GluN1/GluN2C receptor responses to 10 μM L-glutamate and 10 μM glycine and blocked by co-application of 1 μM MK-801 in the absence (left) or presence (right) of 100 μM UBP684. Drug applications are as indicated by the bars above the traces. Scale bars indicate current (nA) and time (sec). (**B**) Left: Normalized trace of MK-801 inhibition in the absence (black) and the presence (green) of UBP684. Right: Normalized trace of NMDAR response inhibition by 10 μM UBP792 in the absence (black) and the presence (green) of UBP684. (**C**) The mean rate of inhibition of GluN1/GluN2C and GluN1/GluN2D responses by MK-801 (left and middle graph) and UBP792 inhibition of GluN1/GluN2D responses (right graph) in the absence (open bars; n = 3 - 6 oocytes) and in the presence (solid bars; n = 4 - 6 oocytes) of 100 μM UBP684 or 50 μM UBP753 as indicated. Data represent mean ± SEM *$p<0.05$, * $p<0.01$.

Figure 9.

UBP684 slows the deactivation time of NMDARs.

(**A**) Receptor deactivation time was studied by removing agonists (10 μM L-glutamate or10 μM glycine) after obtaining GluN1-1a/GluN2D steady-state response with /without UBP753 (50 μM) or UBP684 (50 μM). The deactivation time constant was obtained by fitting a two-component exponential function. A representative trace of agonist deactivation in absence or presence of

UBP684 is shown in the middle and the superimposed, normalized deactivation trace with (green) and without (black) UBP684 is shown on the right (n = 7 - 15 oocytes per group). Data represent mean ± SEM ***p<0.001 (one-way ANOVA followed by Bonferroni's multiple comparison test). (**B**) Deactivation time for glycine removal was studied in presence of L-glutamate and in the presence or absence of UBP684 (green) or UBP753 (red). Traces in the middle show the deactivation kinetics upon glycine removal with (green) and without (black) UBP684. Traces on the right are the corresponding normalized deactivation traces (with UBP684, green; without UBP684, black; n = 5 oocytes per group). Data represent mean ± SEM (**C**) The deactivation time for L-glutamate removal in the presence of glycine and in presence/absence of UBP 684 or UBP753. The trace in the middle shows the deactivation kinetics following L-glutamate removal and the trace on the right is the normalized trace of the deactivation kinetics (n = 6-7 oocytes per group). Scale bar: horizontal = time in sec, vertical = current in nA. Data represent mean ± SEM, *p<0.05 (one-way ANOVA followed by Bonferroni's multiple comparison test).

Figure 10.

Whole cell and single channel recordings in response to rapid agonist application; effects of UBP684 on responses by GluN1/GluN2A receptors expressed in HEK cells.

(**A**) An NMDAR current evoked by a short pulse of Glu (30 μM) with (red trace) or without (black trace) 30 μM UBP684. (**B**) Quantification of the effect of UBP684 on peak amplitude and decay time constant (n = 4). (**C**) Effect on NMDAR single channel currents (representative traces from patch believed to contain only one channel), elicited by a short pulse of Glu. (**D**) An ensemble current (mean) composed of single channel responses as in C with (red) and without (black) 30 μM UBP684.

Figure 11.

Effect of the LBD cleft conformation on potentiation by UBP753.

(**A**) Representative recordings showing the effect of 10 μM L-glutamate (open bar), 10 μM glycine (gray bar), or both agonists (black bar) on wildtype (GluN1/GluN2A), GluN1 LBD-locked (GluN1^{c}/GluN2A) and GluN2A LBD-locked (GluN1/GluN2A^{c}) NMDARs expressed in *Xenopus laevis* oocytes and (lower panel) the effect of 100 μM UBP753 (red bar) on agonist responses in the same three receptors as indicated. Scale bar: horizontal = time in sec, vertical = current in nA. (**B**) Histogram showing the average potentiation by UBP753 of agonist-induced (10 μM L-glutamate and 10 μM glycine) responses from oocytes expressing WT (black, n = 17 oocytes), GluN1 LBD-locked (blue, n = 9 oocytes) and GluN2A LBD-locked (yellow, n = 16 oocytes) receptors. Data represent the mean ± SEM, ****$p<0.0001$ (one-way ANOVA followed by Tukey's multiple comparison test). (**C**) Schematic representing the two cysteine point mutations in the LBD region of GluN1 (N499C and Q686C) leading to the glycine binding site-locked conformation and in the LBD of GluN2A (K487C and N687C) leading to the L-glutamate binding site-locked conformation.

Figure 1

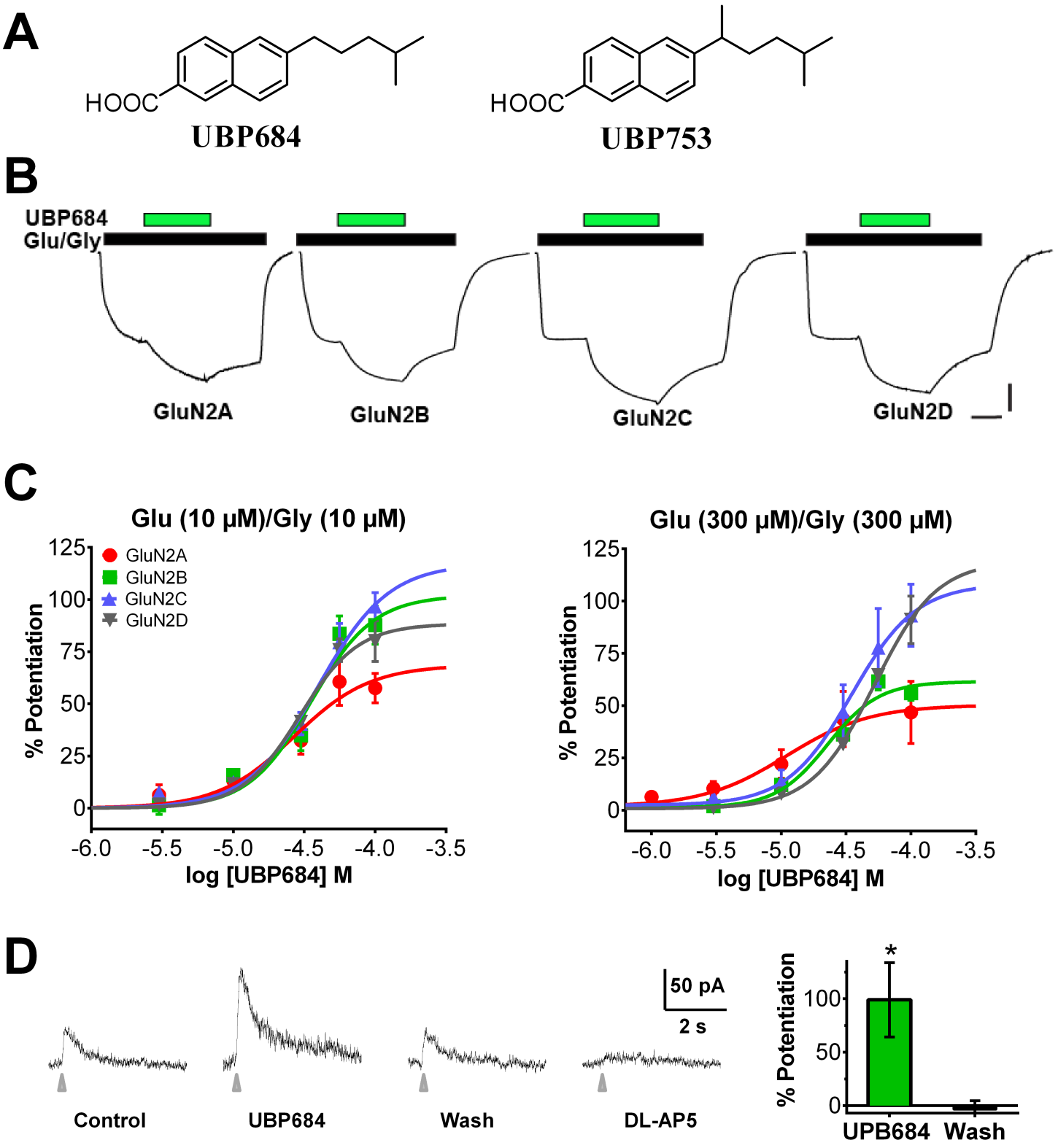
A
HOOC
UBP684
HOOC
UBP753
B
UBP684
Glu/Gly
GluN2A
GluN2B
GluN2C
GluN2D
C
Glu (10 μM)/Gly (10 μM)
GluN2A
GluN2B
GluN2C
GluN2D
% Potentiation
log [UBP684] M
Glu (300 μM)/Gly (300 μM)
% Potentiation
log [UBP684] M
D
50 pA
2 s
Control
UBP684
Wash
DL-AP5
% Potentiation
UPB684
Wash

Figure 2

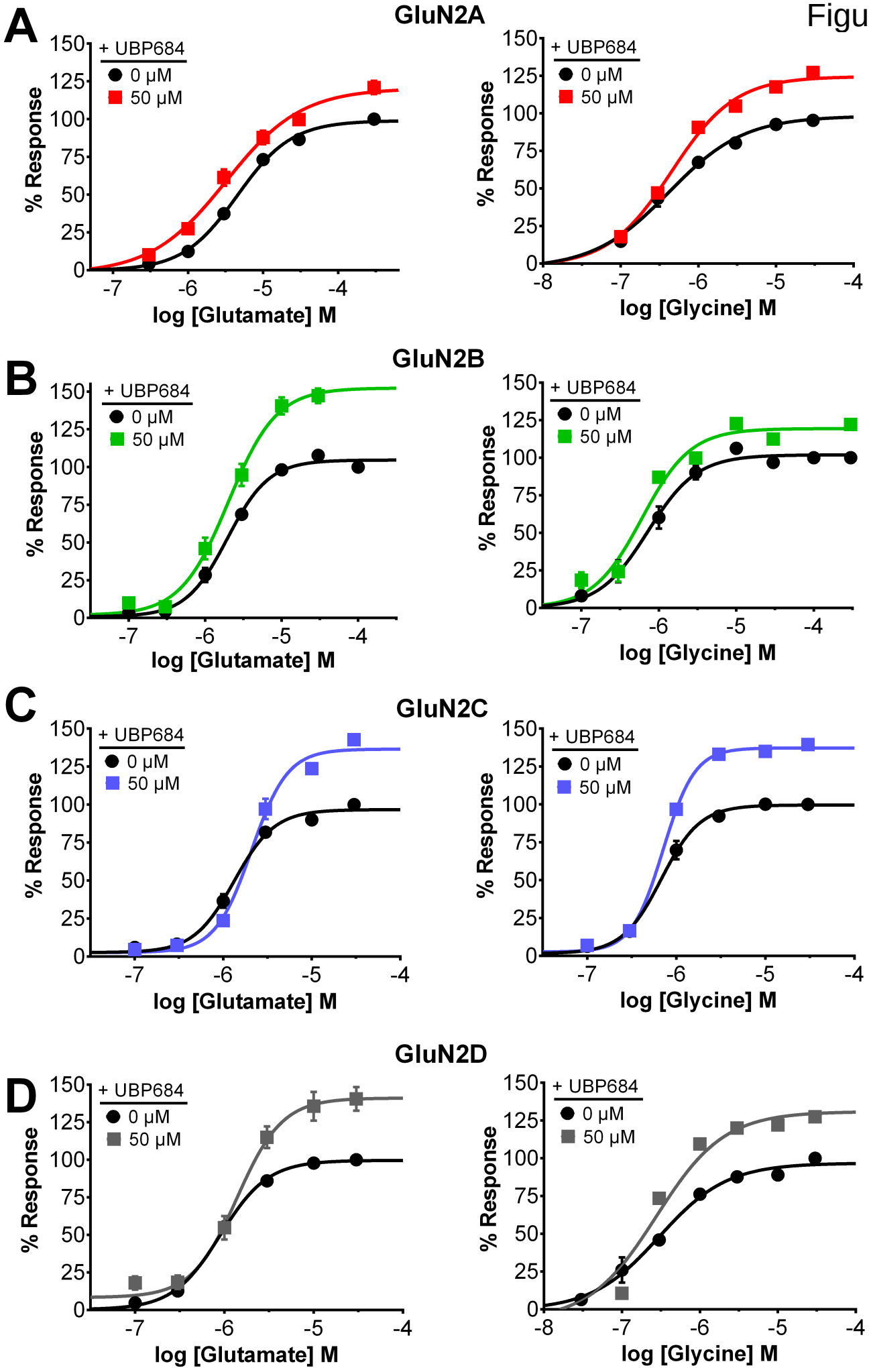
A
GluN2A
+ UBP684
0 μM
50 μM
% Response
log [Glutamate] M
log [Glycine] M
B
GluN2B
C
GluN2C
D
GluN2D

Figure 3

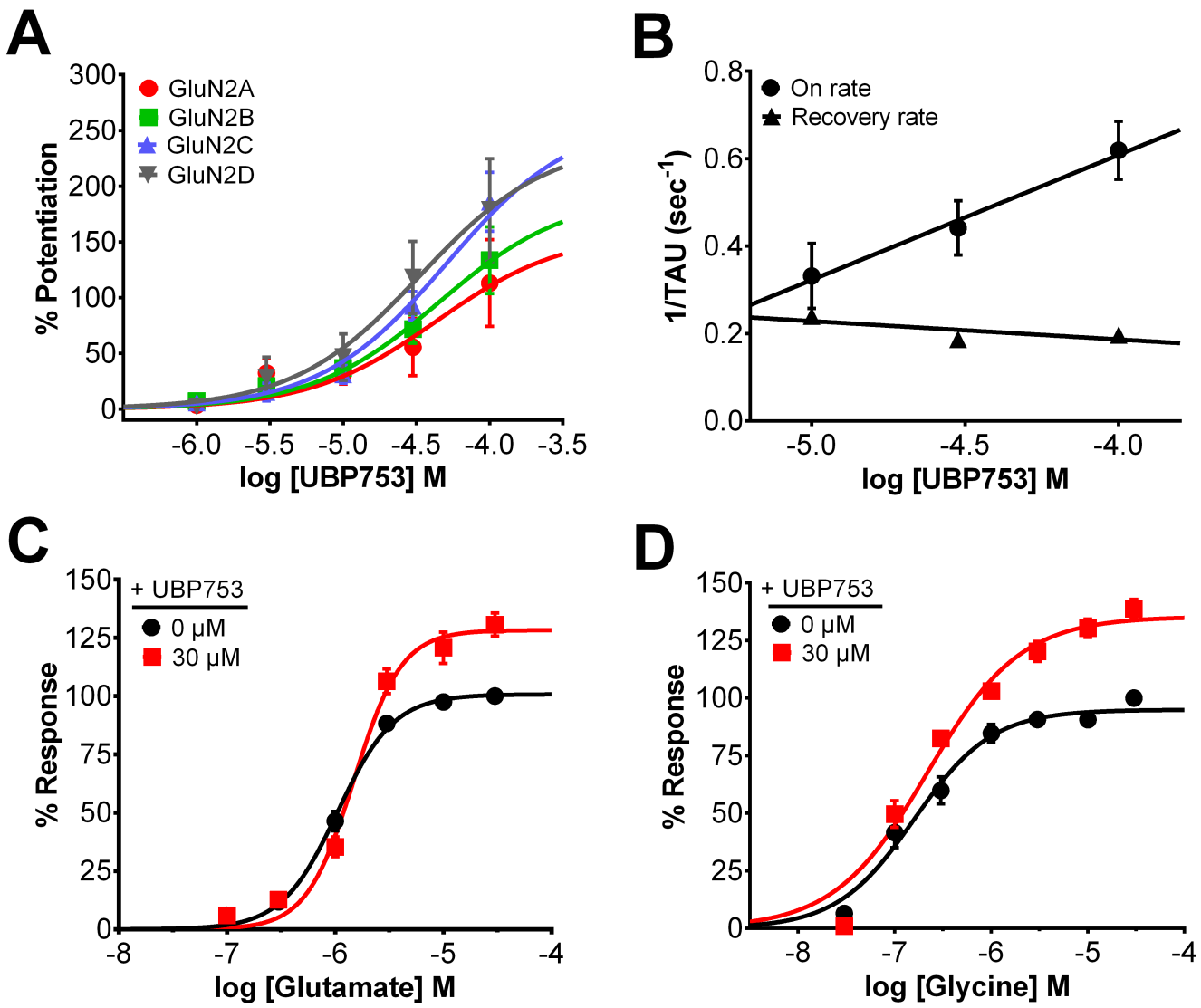
A
300
250
200
150
100
50
0
% Potentiation
GluN2A
GluN2B
GluN2C
GluN2D
-6.0
-5.5
-5.0
-4.5
-4.0
-3.5
log [UBP753] M
B
0.8
0.6
0.4
0.2
0.0
1/TAU (sec-1)
On rate
Recovery rate
-5.0
-4.5
-4.0
log [UBP753] M
C
150
125
100
75
50
25
0
% Response
+ UBP753
0 µM
30 µM
-8
-7
-6
-5
-4
log [Glutamate] M
D
150
125
100
75
50
25
0
% Response
+ UBP753
0 µM
30 µM
-8
-7
-6
-5
-4
log [Glycine] M

Figure 4

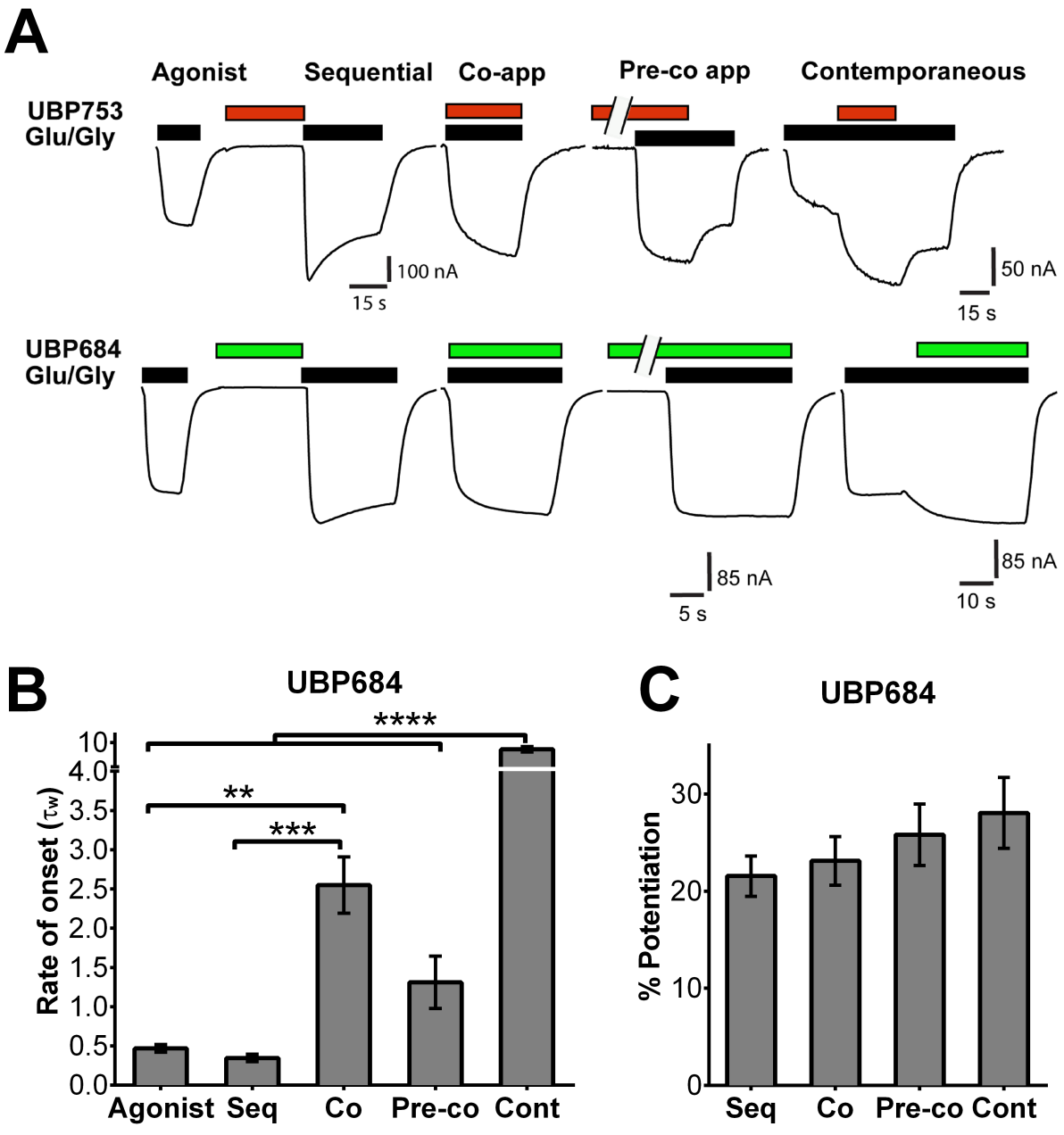
A
Agonist
Sequential
Co-app
Pre-co app
Contemporaneous
UBP753
Glu/Gly
100 nA
15 s
50 nA
15 s
UBP684
Glu/Gly
85 nA
5 s
85 nA
10 s
B
UBP684
Rate of onset (τw)
****
**
***
Agonist
Seq
Co
Pre-co
Cont
C
UBP684
% Potentiation
Seq
Co
Pre-co
Cont

Figure 5

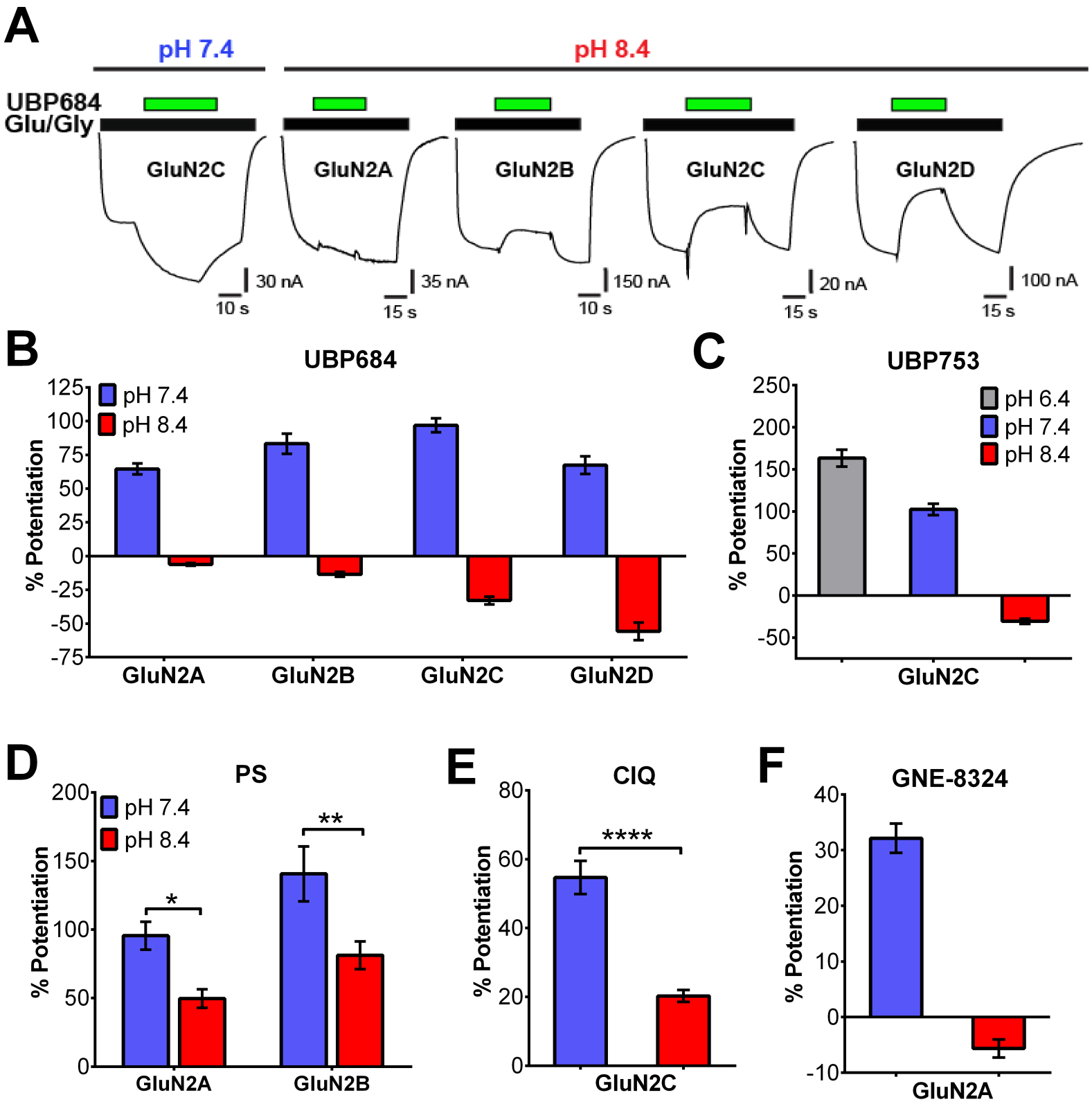
A
pH 7.4
pH 8.4
UBP684
Glu/Gly
GluN2C
GluN2A
GluN2B
GluN2C
GluN2D
30 nA
10 s
35 nA
15 s
150 nA
10 s
20 nA
15 s
100 nA
15 s
B
UBP684
pH 7.4
pH 8.4
% Potentiation
125
100
75
50
25
0
-25
-50
-75
GluN2A
GluN2B
GluN2C
GluN2D
C
UBP753
pH 6.4
pH 7.4
pH 8.4
% Potentiation
250
200
150
100
50
0
-50
GluN2C
D
PS
pH 7.4
pH 8.4
% Potentiation
200
150
100
50
0
*
**
GluN2A
GluN2B
E
ClQ
% Potentiation
80
60
40
20
0
****
GluN2C
F
GNE-8324
% Potentiation
40
30
20
10
0
-10
GluN2A

Figure 6

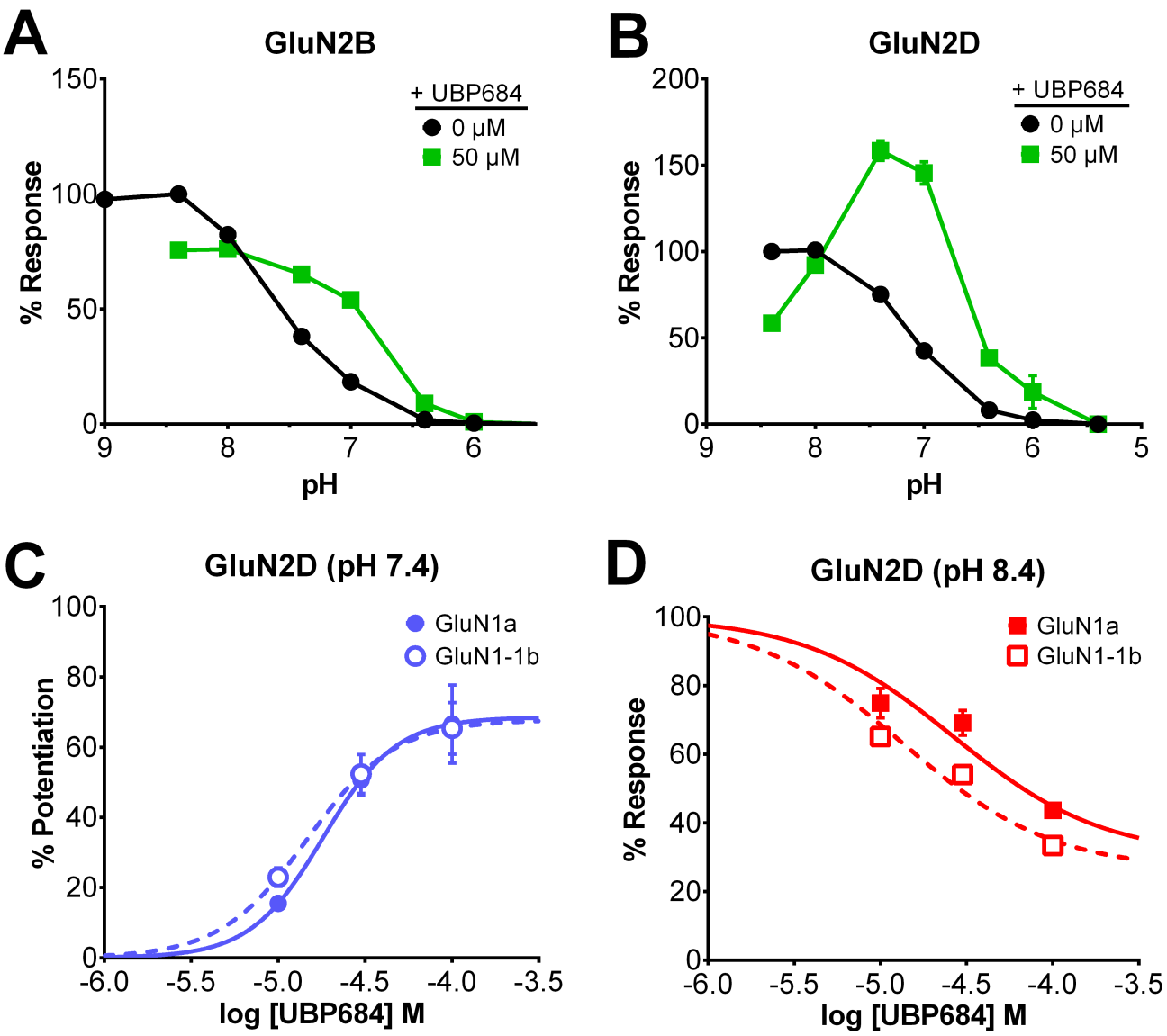
A
GluN2B
+ UBP684
0 μM
50 μM
% Response
pH
B
GluN2D
+ UBP684
0 μM
50 μM
% Response
pH
C
GluN2D (pH 7.4)
GluN1a
GluN1-1b
% Potentiation
log [UBP684] M
D
GluN2D (pH 8.4)
GluN1a
GluN1-1b
% Response
log [UBP684] M

Figure 7

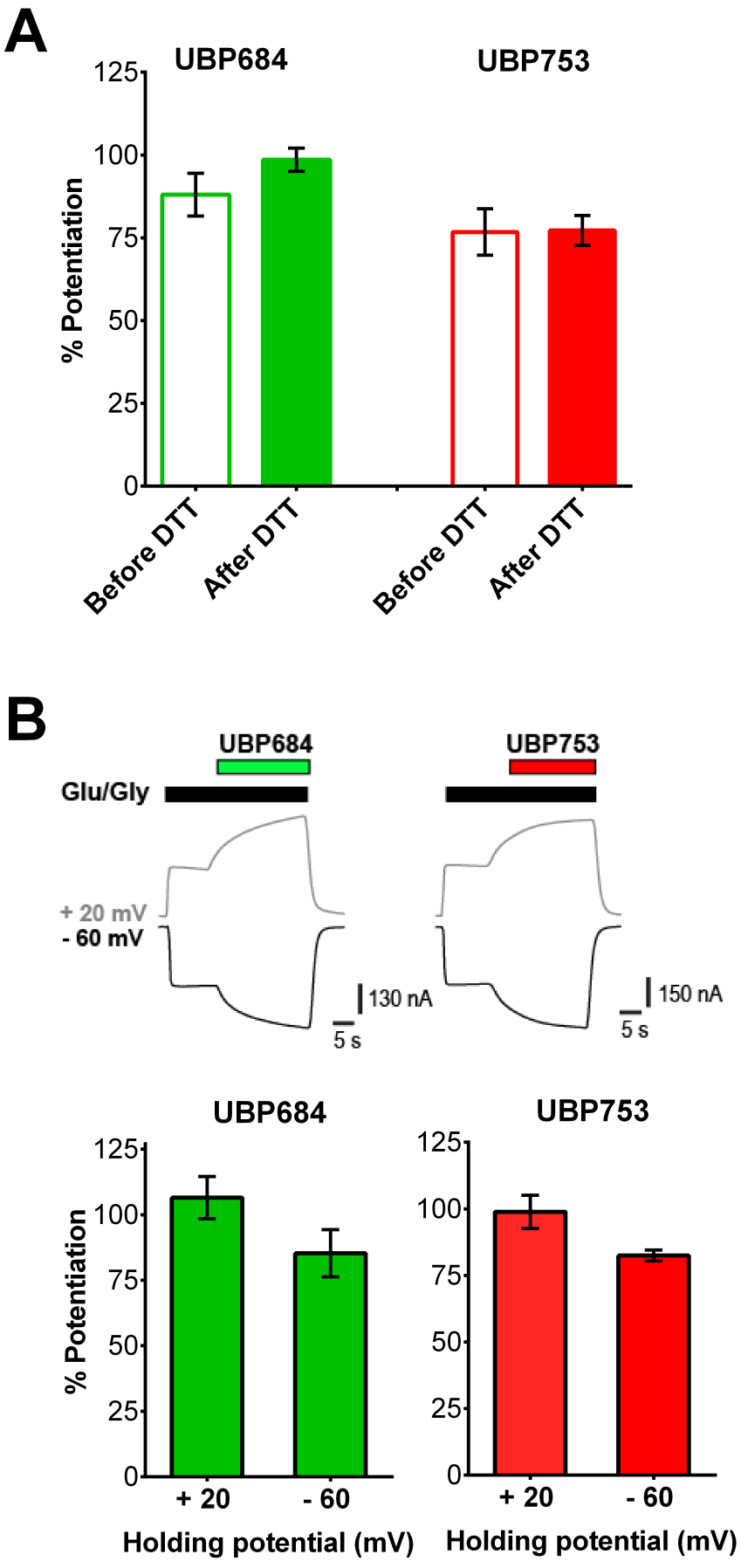
A
UBP684
UBP753
125
100
75
50
25
0
% Potentiation
Before DTT
After DTT
Before DTT
After DTT
B
UBP684
UBP753
Glu/Gly
+ 20 mV
- 60 mV
130 nA
5 s
150 nA
5 s
UBP684
UBP753
125
100
75
50
25
0
% Potentiation
+ 20
- 60
+ 20
- 60
Holding potential (mV)
Holding potential (mV)

Figure 8

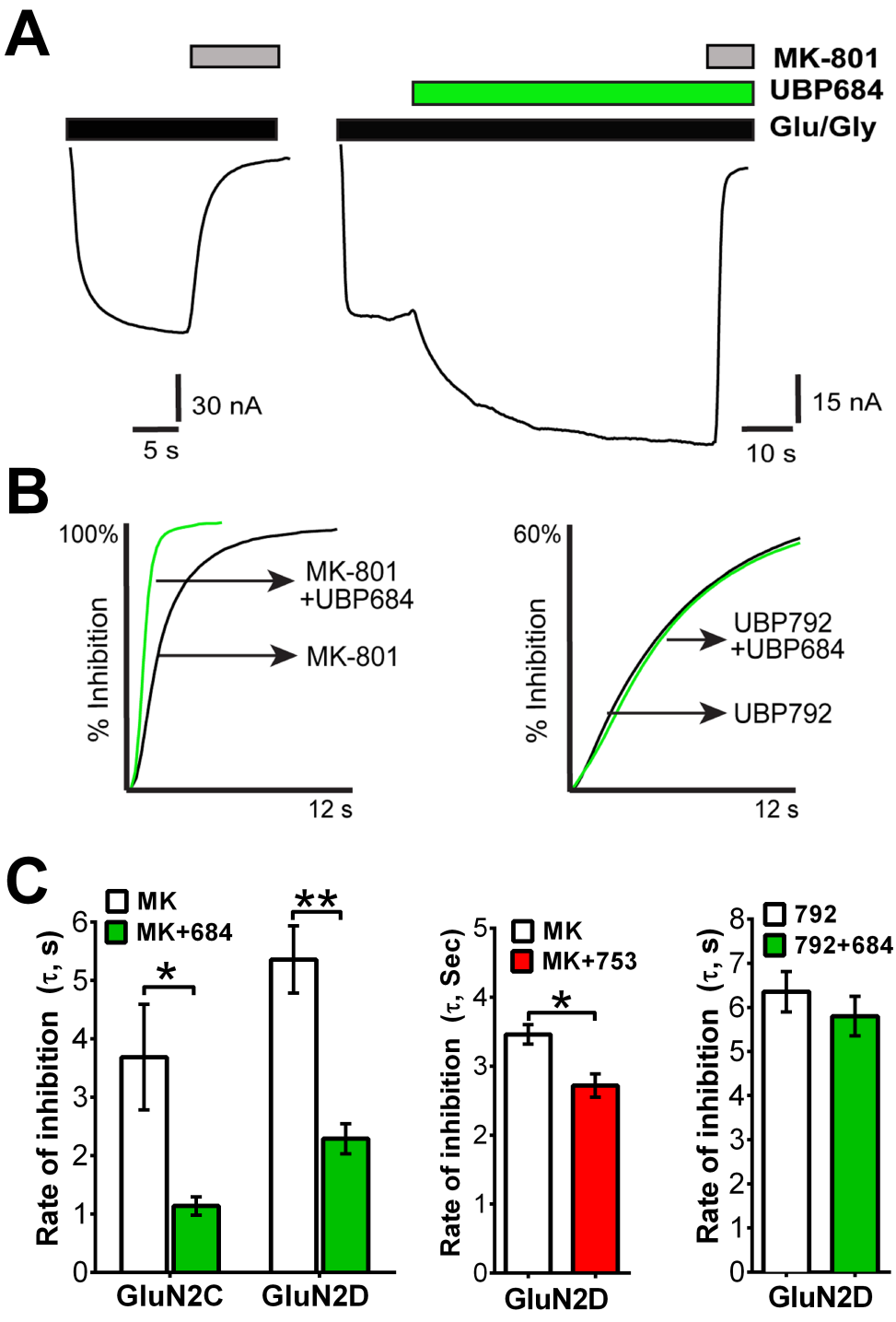
A
MK-801
UBP684
Glu/Gly
30 nA
5 s
15 nA
10 s
B
100%
% Inhibition
MK-801
+UBP684
MK-801
12 s
60%
% Inhibition
UBP792
+UBP684
UBP792
12 s
C
MK
MK+684
Rate of inhibition (τ, s)
GluN2C
GluN2D
MK
MK+753
Rate of inhibition (τ, Sec)
GluN2D
792
792+684
Rate of inhibition (τ, s)
GluN2D

Figure 9

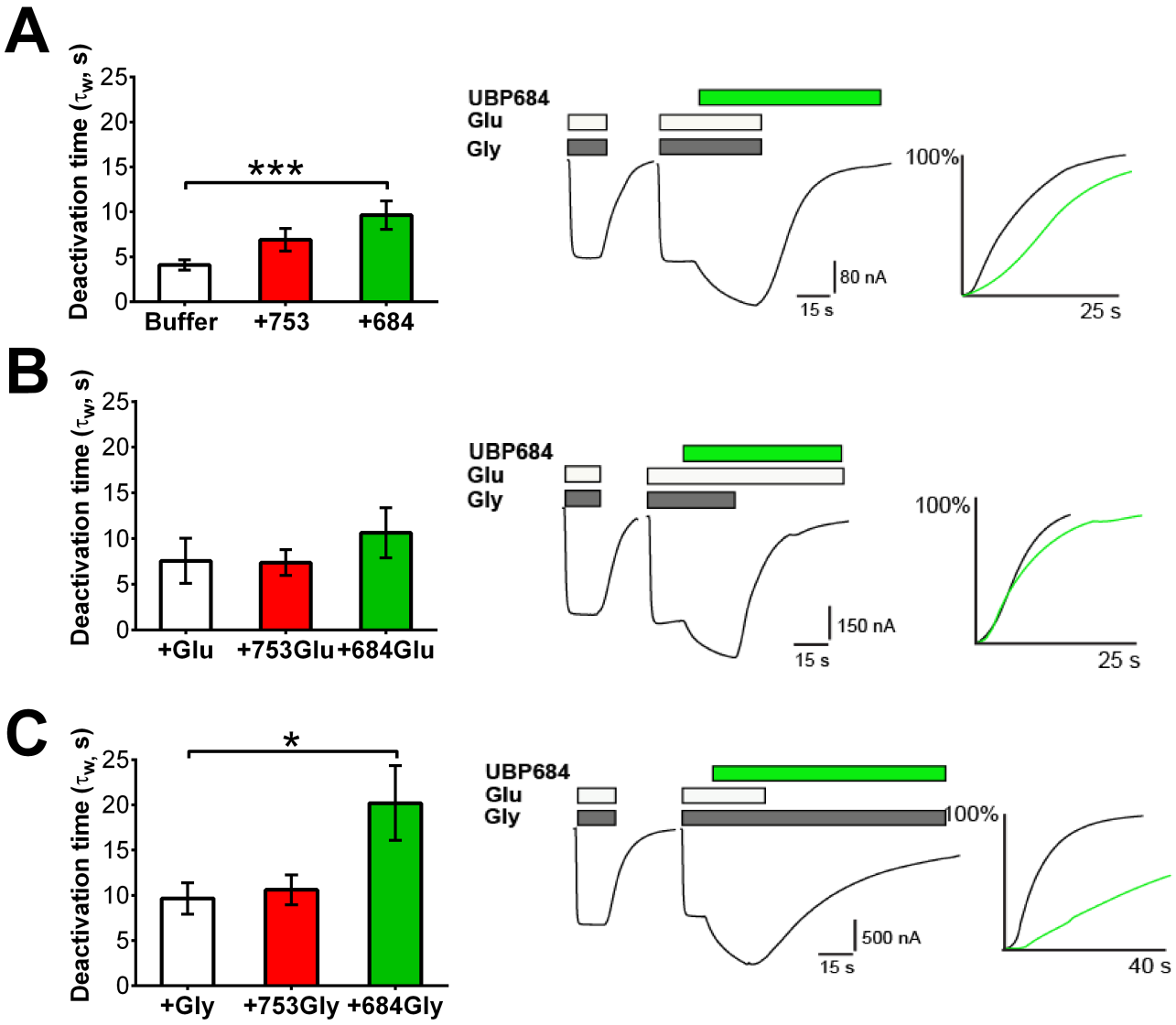
A
Deactivation time (τ_w, s)
25
20
15
10
5
0
***
Buffer
+753
+684
UBP684
Glu
Gly
80 nA
15 s
100%
25 s
B
Deactivation time (τ_w, s)
+Glu
+753Glu
+684Glu
UBP684
Glu
Gly
150 nA
15 s
100%
25 s
C
Deactivation time (τ_w, s)
*
+Gly
+753Gly
+684Gly
UBP684
Glu
Gly
500 nA
15 s
100%
40 s

Figure 10

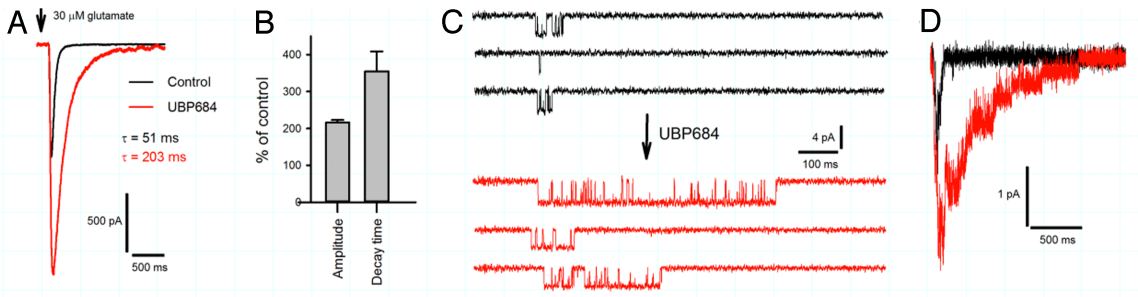
A
30 μM glutamate
Control
UBP684
τ = 51 ms
τ = 203 ms
500 pA
500 ms
B
% of control
400
300
200
100
0
Amplitude
Decay time
C
UBP684
4 pA
100 ms
D
1 pA
500 ms

Figure 11

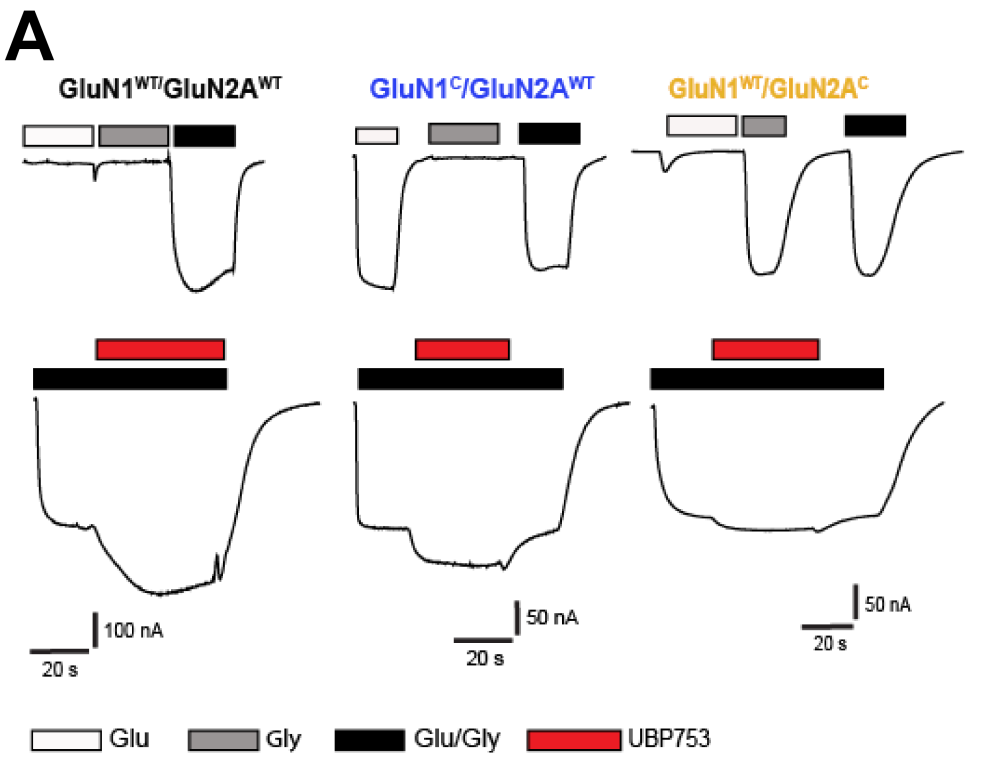
A
GluN1WT/GluN2AWT
GluN1C/GluN2AWT
GluN1WT/GluN2AC
100 nA
20 s
50 nA
20 s
50 nA
20 s
Glu
Gly
Glu/Gly
UBP753

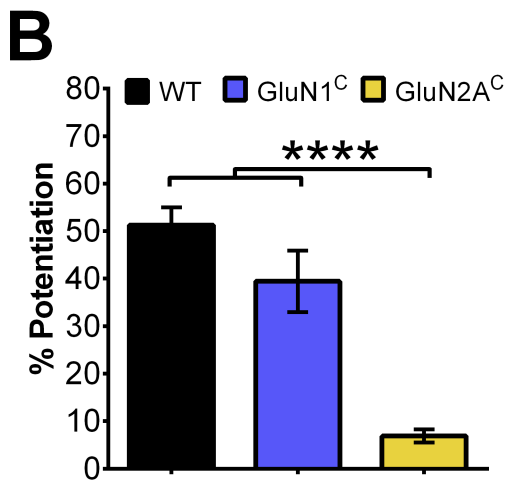
B
WT
GluN1C
GluN2AC
% Potentiation
80
70
60
50
40
30
20
10
0
****

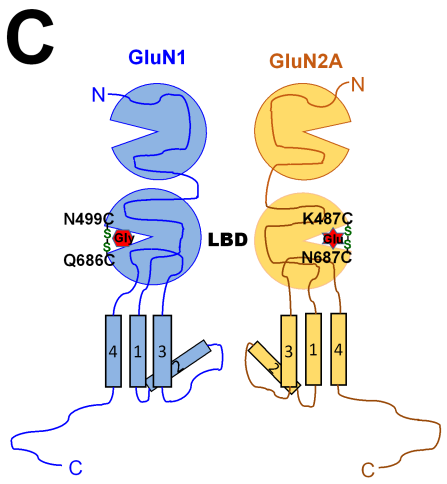
C
GluN1
GluN2A
N
N
N499C
Gly
Q686C
LBD
K487C
Glu
N687C
4
1
3
3
1
4
C
C